Inflammation-associated suppression of metabolic gene networks in acute and chronic liver disease

Archives of Toxicology

Inflammation-associated suppression of metabolic gene networks in acute and chronic liver disease

--Manuscript Draft--

Manuscript Number:	ATOX-D-19-00650R1
Full Title:	Inflammation-associated suppression of metabolic gene networks in acute and chronic liver disease
Article Type:	Original Article
Corresponding Author:	Jan G. Hengstler IfADo Leibniz Research Centre for Working Environment and Human Factors at the Technical University of Dortmund Dortmund, GERMANY
Corresponding Author Secondary Information:	
Corresponding Author's Institution:	IfADo Leibniz Research Centre for Working Environment and Human Factors at the Technical University of Dortmund
Corresponding Author's Secondary Institution:	
First Author:	Jan G. Hengstler
First Author Secondary Information:	
Order of Authors:	Jan G. Hengstler
Order of Authors Secondary Information:	
Funding Information:	FP7 Health (266838) — Prof. Jan G. Hengstler Nottingham City Primary Care Trust (GB) (267038) — Prof. Jan G. Hengstler Helmholtz Virtuelles Institut Multifunktionale Biomaterialien für die Medizin (DE) (0313854) — Prof. Jan G. Hengstler FONDECYT (1140549) — Not applicable
Abstract:	Background & aims Inflammation has been recognized as essential for restorative regeneration. Here we analyzed the sequential processes during onset of liver injury and subsequent regeneration based on time-resolved transcriptional regulatory networks (TRNs) to understand the relationship between inflammation, mature organ function and regeneration.Methods Genome-wide expression and TRN analysis were performed time-dependently in mouse liver after acute injury by CCl 4 (2h, 8h, 1, 2, 4, 6, 8, 16 days) as well as lipopolysaccharide (LPS, 24h) and compared to publicly available data after tunicamycin exposure (mouse, 6h), hepatocellular carcinoma (HCC, mouse), and human chronic liver disease (non-alcoholic fatty liver, HBV infection and HCC). Spatio-temporal investigation differentiated lobular zones for signaling and transcription factor expression.Results Acute CCl 4 intoxication induced expression of gene clusters enriched for inflammation and stress signaling that peaked between 2 and 24h, accompanied by a decrease of mature liver functions, particularly metabolic genes. Metabolism decreased not only in pericentral hepatocytes that underwent CCl 4 induced necrosis but extended to the surviving periportal hepatocytes. Proliferation and tissue restorative TRNs occurred only later reaching a maximum at 48h. The same upstream

	regulators (e.g. inhibited RXR function) initiated increased inflammation and suppressed metabolism. The concomitant inflammation/metabolism TRN occurred similarly after acute LPS and tunicamycin challenges, in chronic mouse models and also in human liver diseases.Conclusions Downregulation of metabolic genes occurs concomitantly to induction of inflammation-associated genes as an early response and appears to be initiated by similar upstream regulators in acute and chronic liver diseases in humans and mice. In the acute setting, proliferation and restorative regeneration associated TRNs peak only later when metabolism is already suppressed.
Response to Reviewers:	..

Inflammation-associated suppression of metabolic gene networks in acute and chronic liver disease

Gisela Campos[1,‡], Wolfgang Schmidt-Heck[2,‡], Jonathan De Smedt[3], Agata Widera[1], Ahmed Ghallab[1,4], Larissa Pütter[1], Daniela González[1], Karolina Edlund[1], Cristina Cadenas[1], Rosemarie Marchan[1], Reinhard Guthke[2], Catherine Verfaillie[3], Claudio Hetz[5,6,7,8], Agapios Sachinidis[9], Albert Braeuning[10,11], Michael Schwarz[10], Thomas S. Weiß[12], Benjamin K Banhart[15], Jan Hoek[15], Rajanikanth Vadigepalli[15], Jeffry Willy[16], James L. Stevens[13], David C. Hay[14], Jan G. Hengstler[1*], Patricio Godoy[1,*]

* *Shared corresponding authors*

‡ Equal contribution

[1] IfADo-Leibniz Research Centre for Working Environment and Human Factors at the Technical University Dortmund, Dortmund, Germany
[2] Leibniz Institute for Natural Product Research and Infection Biology e.V.-Hans- Knöll Institute, Jena, Germany
[3] Stem Cell Institute, KU Leuven, Belgium
[4] Department of Forensic and Veterinary Toxicology, Faculty of Veterinary Medicine, South Valley University, Qena-Egypt
[5] Biomedical Neuroscience Institute, Faculty of Medicine, University of Chile, Santiago, Chile
[6] Center for Geroscience, Brain Health and Metabolism (GERO), Santiago, Chile
[7] The Buck Institute for Research in Aging, Novato CA 94945, USA
[8] Department of Immunology and Infectious Diseases, Harvard School of Public Health, Boston, Massachusetts, United States of America
[9] Institute of Neurophysiology, Medical Faculty, University of Cologne, Cologne, Germany
[10] University of Tübingen, Dept. of Experimental and Clinical Pharmacology and Toxicology, Tübingen, Germany
[11] Federal Institute for Risk Assessment, Dept. Food Safety, Max-Dohrn-Str. 8-10, 10589 Berlin, Germany
[12] Center for Liver Cell Research, Department of Pediatrics and Juvenile Medicine, University of Regensburg Hospital, Regensburg, Germany
[13] Lilly Research Laboratories, Eli Lilly and Company, Lilly Corporate Center, Indianapolis, IN 46285, USA
[14] MRC Centre for Regenerative Medicine, University of Edinburgh, Edinburgh, United Kingdom, EH16 4UU
[15] Department of Pathology, Anatomy, and Cell Biology, Thomas Jefferson University, Philadelphia, PA USA
[16] Vertex Pharmaceuticals 3215 Merryfield Row, San Diego, CA 92121, USA

Contact information

Patricio Godoy, IfADo-Leibniz Research Centre for Working Environment and Human Factors at the Technical University of Dortmund. Ardeystrasse 67, 44139, Dortmund, Germany. Tel. ++49-0231-108-4370; Fax: ++49-0231-108-4403; email godoy@ifado.de

Keywords – Liver injury, regeneration, transcriptomics, gene networks

Word count - Abstract 250; Introduction 673; Materials and Methods 26; Results 2,379; Discussion 1,111; Fig legends 611; References 878

Number of figures – 6

Number of tables – none

Conflict of interest statement – Nothing to disclose

Financial support - This study was supported by the European Union Seventh Framework Programme (FP7)-Health projects DETECTIVE (EU-project FP7-Health Grant Agreement No. 266838) and NOTOX (EU-project FP7-Health Grant Agreement No. 267038) (JGH), the DFG WISP (GO 1987/2-1) (PG), the BMBF (German Federal Ministry of Education and Research) project Virtual Liver (0313854) (JGH), FONDECYT no. 1140549, Millennium Institute No. P09-015-F and FONDAP 15150012 (CH).

Authors contributions - GC, AW, AG, LP, - mouse experiments with CCl_4, Tm and LPS challenge; GC, AW, LP –western blot analyses; GC – histological analysis; WSC, PG, JdS and AS – gene array analysis and bioinformatics; AB and MS – zonated gene array analysis; GC, DG – real time PCR analysis; GC, JGH and PG – drafting of manuscript, acquisition of funding; GC, JGH and PG – Study concept and design, critical review of manuscript, study supervision; KE, CC, RM, RR, RG, CV, CH, MS, TSW, JLS, DCH and DD - Study concept and design, critical revision of manuscript.

List of abbreviations

HCC: hepatocellular carcinoma; NAFLD: non-alcoholic fatty acid liver diease; TRN: transcriptional regulatory networks; IPA: Ingenuity pathway analysis; Tm: tunicamycin; LPS: lipopolysaccharide; HBV: hepatitis virus type B

Acknowledgements

We thank Ms. Katharina Rochlitz, Ms. Brigitte Begher-Tibbe and Ms. Georgia Günther (Leibniz Research Centre for Working Environment and Human Factors, Technical University of Dortmund, Germany) for excellent technical assistance. This work has received funding from the European Union's Horizon 2020 research and innovation programme under grant agreement No 681002 (EU-ToxRisk), from TransQST (No. 116030), LivSysTransfer (BMBF, 031L0119) with contributions from StemCellNet (BMBF, 01EK1604A), LiSyM (BMBF, 031Loo45) and InnoSysTox (BMBF/EU, 031L0021A) We thank the Permanent Senate Commission on Food Safety (SKLM) for valuable discussion.

Abstract

Background & aims: Inflammation has been recognized as essential for restorative regeneration. Here we analyzed the sequential processes during onset of liver injury and subsequent regeneration based on time-resolved transcriptional regulatory networks (TRNs) to understand the relationship between inflammation, mature organ function and regeneration.

Methods: Genome-wide expression and TRN analysis were performed time-dependently in mouse liver after acute injury by CCl_4 (2h, 8h, 1, 2, 4, 6, 8, 16 days) as well as lipopolysaccharide (LPS, 24h) and compared to publicly available data after tunicamycin exposure (mouse, 6h), hepatocellular carcinoma (HCC, mouse), and human chronic liver disease (non-alcoholic fatty liver, HBV infection and HCC). Spatio-temporal investigation differentiated lobular zones for signaling and transcription factor expression.

Results: Acute CCl_4 intoxication induced expression of gene clusters enriched for inflammation and stress signaling that peaked between 2 and 24h, accompanied by a decrease of mature liver functions, particularly metabolic genes. Metabolism decreased not only in pericentral hepatocytes that underwent CCl_4 induced necrosis but extended to the surviving periportal hepatocytes. Proliferation and tissue restorative TRNs occurred only later reaching a maximum at 48h. The same upstream regulators (e.g. inhibited RXR function) were implicated in increased inflammation and suppressed metabolism. The concomitant inflammation/metabolism TRN occurred similarly after acute LPS and tunicamycin challenges, in chronic mouse models and also in human liver diseases.

Conclusions: Downregulation of metabolic genes occurs concomitantly to induction of inflammation-associated genes as an early response and appears to be initiated by similar upstream regulators in acute and chronic liver diseases in humans and mice. In the acute setting, proliferation and restorative regeneration associated TRNs peak only later when metabolism is already suppressed.

Introduction

Inflammation serves to initiate tissue repair by elimination of the causes of injury, such as infectious agents and necrotic cells (Karin et al., 2016; Campos et al., 2014). In recent years, computational modeling of transcriptional regulatory networks (TRNs) as regulatory interactions among transcription factors and their target genes has been used to gain insight into genome-wide expression patterns associated with inflammation and have established a link between inflammatory and regenerative responses (Karin et al., 2014; Michalopoulos, 2013). However, a time-resolved genome-wide analysis of acute inflammation of the liver and a comparison to chronic liver diseases in mouse and human has not yet been performed. To gain deeper insight, we generated time-resolved genome-wide expression data using the well-established protocol of acute injury and inflammation induced by CCl_4 in mouse liver. TRNs obtained in this mouse model were compared to chronic liver inflammation in mouse and human liver tissue, including NAFLD, cirrhosis, HBV infection and HCC. We report a common feature in all acute and chronic liver conditions, namely upregulation of inflammation associated genes that is accompanied by strong downregulation of a large set of genes responsible for mature parenchymal functions, predominantly metabolism. Inflammation-associated downregulation of mature tissue functions is mediated by a similar set of upstream regulators in mouse and human.

Materials and methods

A detailed description of all methods including data processing and visualization, fuzzy clustering and gene set enrichment analysis, ingenuity pathway analysis, immunostaining and microscopy, western blot, RNA isolation, cDNA synthesis, real time quantitative PCR, and mouse experiments are described in Supplement 1. Briefly, differentially expressed genes in mouse liver after acute CCl_4 intoxication with 1.6 g/kg (intraperitoneal) were determined using Affymetrix A450 2.0 gene chips, (Array Express E-MTAB-24445). Liver tissue specimens were collected from five C57BL6/N male mice 2h, 8h, day 1, 2, 4, 6, 8 and 16 after CCl_4 intoxication. Control liver tissue was obtained from mice on day 1 after receiving vehicle (olive oil) intraperitoneal injections. Inflammation-dependent differentially expressed genes were identified by analysis of mouse liver tissue 24h after intraperitoneal administration of lipopolysaccharide (750 ng/kg). Moreover, the following expression data sets were used: mouse liver tissue 6h after intraperitoneal administration of tunicamycin (1 mg/kg) (GSE29929); pericentral (PC) and periportal (PP) enriched hepatocytes; hepatocellular carcinoma (GSE30485); gene array data from human liver tissue: non-alcoholic fatty liver disease (NAFLD, score 0-1, 3-4) (GSE49541); liver tissue infected with hepatitis B (GSE14668); liver cirrhosis and human hepatocellular carcinoma (GSE17548). An overview of the expression data used in the present study is given in **Fig. 1**. Tables containing differentially expressed genes and biostatistical raw data of all data sets are available in Supplements 2-17. Legends giving an overview over all Supplements are given in Supplement 1.

Clusters of correlated genes based on similar time-dependent fold change after CCl_4 intoxication were generated by fuzzy c-means clustering with the fuzziness m=2. To cluster the gene expression profiles of DEGs, their profiles were logarithmised and scaled between the values -1 and 1. The optimal number of clusters was estimated using the 'Separation index'. A gene is assigned to the cluster with the highest degree of membership and if the maximum degree of membership is less than 0.3, the gene is regarded as unassignable and assigned to the group of outliers. A list with the genes contained in each cluster and the respective expression change can be found in the supplemental section.

Results

Inflammation-associated suppression of mature liver functions

To understand the TRNs activated in acute liver injury, we performed a time-resolved Affymetrix gene array study on mouse liver after acute intraperitoneal administration of CCl_4 (1.6 g/kg in olive oil) (Campos et al., 2014) (**Fig 1A;B**; Suppl. Fig. 1 in Supplement 1). In total, 3,750 differentially expressed genes were identified (1.5 fold, $p < 0.05$; FDR adjusted) (Supplement 2). Principal component analysis (PCA) showed clear differences to controls and good clustering of time-matched liver tissue replicates at 2h, 8h, and on days 1, 2 and 4 after CCl_4 administration; at days 6, 8 and 16, expression data were similar to controls again (**Fig 1B**). The high reproducibility between replicates offered good conditions for a time-resolved bioinformatics analysis. Consequently, the fuzzy-c means algorithm was applied which revealed eight time-dependent gene clusters including 3,655 genes (**Fig. 2**) (Supplement 3).

Overrepresented Gene Ontology (GO) and KEGG pathway annotations were used to identify biological motifs associated with time-dependent progression of transcriptional alterations (**Fig 2** and Supplement 4). Because similar genes and enriched GO/KEGG terms were present in some of the eight gene clusters, we joined them into three cluster groups. **Cluster group 1** included upregulated genes that peaked between 2 and 24h (**Fig. 2**, clusters 1a-d). This cluster group contained genes associated with inflammation, cell stress, and the unfolded protein response (UPR). The earliest induced genes (maximal expression at 2h; cluster 1a) were enriched for the MAPK and TNF pathways, while subsequent clusters were mostly enriched in inflammation and ER stress/proteostasis associated genes. Cluster group 1 included multiple intracellular signaling components and transcription factors (e.g. Gadd45g, Jun, Atf4, Maff) as well as growth factors and cytokines (e.g. Fgf21, Cxcl1, Ccl2, Ccl6) (**Fig 2**).

Cluster group 2 included downregulated genes that reached a minimum of expression at 8 and 24h upon CCl_4 administration, thereby responding in the same time interval as the upregulated genes of cluster group 1 (**Fig. 2**; clusters 2a-b). Cluster group 2 was enriched in genes associated with mature liver function, particularly metabolism; it included the GO annotations “Small molecule metabolic process”, “Organic acid metabolic process”, and the KEGG pathways “Valine, leucine and isoleucine

degradation", "Steroid hormone biosynthesis" and "Drug metabolism-cytochrome P450". Selected individual genes from the different cluster groups were validated by qRT-PCR (Suppl. Fig. 2 in Supplement 1). Together, cluster groups 1 and 2 showed a time-resolved transient induction of genes associated with stress signaling, inflammation and ER stress that occurred simultaneously with a massive downregulation of genes associated with metabolism and further functions of the mature liver.

Cluster group 3 genes responded later than the genes of cluster groups 1 and 2, showing maximal expression not before day 2 after CCl_4 intoxication (**Fig. 2**, clusters 3a-b). These clusters represent genes associated with proliferation, wound healing and immune cell infiltration. They correspond to GO terms such as "Cell cycle", "ECM organization" and "Immune response", and the KEGG terms "DNA replication".

Identification of TRNs in acute liver injury and regeneration

Having identified the most significant biological motifs activated during liver injury and regeneration, we sought to establish the TRNs controlling the aforementioned time-dependent gene clusters. KEGG pathway enrichment analysis provided only little insight into the critical TRNs controlling the deregulated genes. Therefore, a more accurate representation of TRNs was established by identifying 1) deregulated transcription factors, 2) overrepresented transcription factor binding sites (TFBS) in the promoter/enhancers (Supplement 4), and 3) upstream regulator inference using ingenuity pathway analysis (IPA) (Supplement 5). These approaches revealed tremendous details of TRNs components in each cluster group (**Fig 2**). For example, TFs upregulated in Cluster group 1 included well-known stress regulators, such as Fos, Jun, Cebpb, and Egr1, as well as TFs that have not yet been associated with acute liver injury, including Klf10, Klf6, Ybx3 and Sox9. Cluster group 2 contained downregulated TFs with known roles in metabolic functions of healthy liver, such as Nr0b2 (SHP), Nr1h4 (FXR), Nr1l2 (PXR) and Cebpa, and TFs with no known function in liver metabolism, for example Esr1, Zfp871 and Nr1d1 (Supplement 5).

TFBS enrichment and IPA analysis provided additional information on transcriptional regulators whose expression is not transcriptionally altered during acute

liver injury. For example, TFBS overrepresented in Cluster groups 1 included HIF-1, AHR/HIF, Foxp1, ETF and Elk-1 (**Fig 2** and Supplement 5). Cluster group 2 was enriched in HNF4 and HNF1 TFBS. Further TRN modulators were identified in Cluster groups 1 by IPA, including ER stress signaling members Xbp1 (activated by splicing), Eif2AK3 (PERK) and ERN1 (IRE1a) (activated by phosphorylation), Ikbkb and Nfe2l2 (activated by proteolytic cleavage) and Nr1l3 (CAR) (activated by ligand engagement) in (**Fig 2** and Supplement 5). In Cluster group 2 IPA revealed well-known regulators of liver metabolism (e.g. HNF4, PPARA, SREBF1 and 2, and PPARG), and regulators associated with upregulated gene clusters, such as TNF and MAP4K4 (**Fig 2** and Supplement 5).

Characterization of spatio-temporal signaling during CCl_4-induced liver injury

To investigate the spatio-temporal relationships of signaling in liver parenchyma, immunohistochemical analysis of transcription factors in liver sections of CCl_4 treated mice was performed. First, we focused on Cluster group 1 factors c-Jun and CEBPD. c-Jun expression was not detected in control tissues, but increased in hepatocyte nuclei, particularly in PC hepatocytes 2h after CCl_4 administration (**Fig 3A**; Suppl. Fig. 3 in Supplement 1). On day 1, when the dead cell area is clearly discernible, c-Jun staining slightly exceeded the PC dead area, but never reached periportal hepatocytes (**Fig 3A**). This is comparable to the PC expression of the ER-stress associated transcription factor CHOP after CCl_4 intoxication (Suppl. Fig. 4 in Supplement 1 and [2]). The inflammation-associated transcription factor CEBPD from Cluster group 1A exhibited a different response (**Fig 3A**). At 2h, nuclear staining was already evident in both the PC and PP hepatocytes. To assess control mechanisms of Cluster group 2 genes, we analyzed expression of HNF4, which showed an inverse expression pattern to the stress and inflammation markers c-Jun and CEBPD. HNF4 was expressed in all hepatocytes of control mice (**Fig 3A**). After 8h CCl_4 treatment it decreased in the PC region and after 24h reached a similarly low level all over the liver lobule. In summary, stress signaling by c-Jun and CHOP occurred predominantly in pericentral hepatocytes, while CEBPD and HNF4, regulatory factors of inflammation and metabolism, were altered in all lobular zones.

The suppression of HNF4 in all lobular zones suggests that metabolic liver functions were not only affected in pericentral hepatocytes, which will undergo necrosis, but also PP hepatocytes. To systematically assess this hypothesis, we analyzed genes from PP and PC enriched hepatocytes (Braeuning et al., 2006) (Supplement 6). Venn diagram analysis of the zonated genes (either expressed in PP or in PC hepatocytes) indicated the largest overlaps with clusters 2a and 2b (**Fig. 3B**; Supplements 7, 8). Noteworthy, the genes with the highest PP-to-PC ratio were among those overlapping with Cluster group 2 genes. CCl_4 does not cause cytotoxicity to PP hepatocytes, because in contrast to PC cells, they do not express Cyp2e1, which is required for metabolic activation of CCl_4. Therefore, the strong expression alterations in the PP cells may represent an adaptation to PC hepatocyte death. In contrast to the genes downregulated in response to CCl_4, zonal genes minimally overlap with upregulated genes in cluster groups 1 to 3 (**Fig 3B**). In conclusion, spatiotemporal analysis reveals zonated (stress) versus non-zonated (inflammation and metabolism) signaling motifs during acute liver injury.

Since cluster 1a (**Fig. 2**) suggested increased stress signaling, e.g. via Fos, Jun, STAT and MAPK, Western blot analyses were performed. A transient increase in pSTAT3, pAkt, pJNK and pERK was evident already 2h after CCl_4 injection (**Fig. 3C**). A biphasic behavior for pAkt and pERK was observed, with a second peak on day 1 for pAkt and day 2 for pERK (**Fig 3C**; quantifications: Suppl. Fig 3 in Supplement 1). These results correspond to the aforementioned Cluster group 1 stress signaling networks. Similarly, the proliferation marker PCNA peaked on days 2 and 4 (**Fig 3C**), in agreement with the timing of the wound healing gene networks (Cluster group 3). Cell stress is often accompanied by increased autophagy. To assess possible alterations in autophagy during CCl_4 intoxication, the autophagosome factors LC3 and p62 were analyzed. Conversion of LC3-I to LC3-II was observed between 2h and day 1 after CCl_4 administration (**Fig 3D**); concurrently the cargo protein p62 and poly-ubiquitinated proteins accumulated between 2 and 24h after CCl_4, suggesting an altered autophagic flux.

Inflammation/ER stress and metabolic gene networks are influenced by the same upstream regulators

When all genes were plotted time-dependently, an almost mirror-inverted pattern was obtained for up- and downregulated genes up to approximately 4 days after CCl_4 administration (**Fig 4A**). Downregulation (similar as upregulation) occurred already at the earliest tested time period of 2h, when pericentral hepatocytes are not yet necrotic. Therefore, decreased gene levels during this time period are unlikely to result from degradation of pericentral liver tissue but rather are due to an active process. To identify possible transcriptional regulatory motifs controlling the up and downregulation of these genes, we first analyzed individual time points during the early phase of stress and injury (2h till day 1) using all differentially expressed genes at each time point. The top ten pathways detected by IPA were related to inflammation, unfolded protein response and metabolism (**Fig 4B**). The most significantly enriched pathway identified at 8h and day 1 was “LPS/IL-1 mediated inhibition of RXR function” (Supplement 9). Similarly, analysis of upstream regulators showed a strong activated score for regulators of inflammation and ER-stress while regulators of liver metabolic functions were estimated as highly inactive (**Fig. 4C** and Supplement 10).

A key result was that the strongest enriched canonical IPA pathway, “LPS/IL-1 Mediated Inhibition of RXR Function” included both highly upregulated inflammation associated gens and downregulated genes associated with mature liver functions (**Fig. 4D**). For example, the inflammation mediating pathway c-Jun was the strongest up and the apical bile salt export carrier BSEP, representing a function of the mature liver, was among the strongest downregulated genes both triggered by the same canonical pathway. Similar principles were also obtained for other canonical pathways, e.g. “Unfolded protein response” triggered upregulation of the hepatocyte transcription factor CEBPB, while CEBPA and SREBF1 were downregulated (**Fig. 4D**). Therefore, activation of inflammation- (and/or ER stress) and suppression of metabolism genes after CCl_4 intoxication may be caused by the same upstream regulators and canonical pathways (**Fig. 4B-D**).

To study if the observations made in CCl_4 intoxicated mice apply also to further models of hepatotoxicity, we analyzed in vivo interventions with LPS (inflammation) and

tunicamycin - Tm (ER stress) under conditions where (in contrast to the CCl_4 protocol) only little necrosis is induced, using previously reported gene array studies (Supplement 11). A highly significant overlap of downregulated genes in LPS and Tm versus CCl_4 treated livers (**Fig. 4E**) was observed, which were enriched in KEGG pathways and GO terms representing metabolism, such as “small molecule catabolic process”, “Steroid metabolic process”, “Drug metabolism-cytochrome P450”, and “PPAR signaling pathway” (**Fig 4F** and Supplement 12). These results indicate that gene networks activated by inflammation (LPS) and/or ER-stress (Tm) trigger downregulation of genes responsible for metabolic functions in the liver, similar to the CCl_4 model.

Inflammation-dependent suppression of metabolic networks in chronic liver disease in mice and human

The presented gene network analysis suggests that inflammation and ER stress may simultaneously induce upregulation of inflammation-associated and downregulation of metabolic gene networks in an injured liver. Noteworthy, during acute injury hepatocytes express markers of embryonic development, such as alpha-fetoprotein (Supplement 2). These features are also observed in immature hepatocytes, such as hepatoblasts and stem cell-derived hepatocytes (Godoy et al., 2015). Because dedifferentiation towards a more immature phenotype is also a feature of hepatocellular carcinoma – HCC, we assessed whether similar inflammation (and ER stress)-induced suppression of metabolic networks occurs in HCC. For this, we analyzed previously generated data of HCC that was induced in mouse livers by a single injection of diethylnitrosamine (DEN) followed by repeated injections of CCl_4 (Liu et al., 2015) (Supplement 13). Spearman correlation analysis of HCC and liver tissue after CCl_4 for all genes showed a high correlation, particularly on days 1 and 2 after CCl_4 (**Fig 5A**). The strong overlap between the chronic and acute liver injury model was observed for up- and downregulated genes (**Fig. 5B**). To identify possible commonalities in gene regulatory networks in both models, we analyzed HCC and acute-injured liver gene expression by IPA (Supplement 14 and 15). The top scoring canonical pathway for HCC and acute CCl_4 intoxication was “LPS/IL-1 mediated inhibition of RXR function” (**Fig 5C** and Supplement 14), with highly significant pathways representing inflammation and liver metabolic networks. Upstream regulators

and their active/inactive states were also similar for HCC and acute CCl_4 intoxication, and known regulators of liver metabolic functions, such as ACOX1, TSC2, mir-122 SCAP, HNF4 and SREBF1 were strongly suppressed (**Fig 5D** and Supplement 15). Activated ER-stress pathways were not detected in experimental HCC, suggesting that inflammation rather than ER stress promotes the suppression of metabolic gene networks in this model.

To establish whether the aforementioned upregulation of inflammation/ER stress and concomitant downregulation of metabolism associated genes also occurs in human liver disease, we analyzed pathways and upstream regulators by IPA in previously reported gene array studies on nonalcoholic fatty liver disease (NAFLD) (Moylan et al., 2014), hepatitis B infection (HBV) (Farci et al., 2010) and HCC (Arai et al., 2010) (**Fig 6** and Supplement 16 and 17). Similar to the acute injury/HCC situation, the most significant IPA pathways in chronic human liver disease were related to liver metabolism (e.g. 'FXR/PXR activation', 'LXR/RXR activation'), as well as inflammation (e.g. 'coagulation system', 'LPS/IL-1 Mediated Inhibition of RXR function') (**Fig 6A** and Supplement 16). These scores were higher in HBV and HCC compared to NAFLD. The pathways were composed of up and downregulated genes. For example, among the top upregulated genes were cytokines (IL-18, IL-33), while downregulated genes included P450 enzymes (e.g. Cyp7a1, Cyp2c8), transporters (e.g. Slco1b3), and TFs (e.g. CAR) (**Fig. 6B-C**). Similar to the mouse models, upstream regulator analysis demonstrated a decrease in mature liver function factors, such as HNF4, HNF1A and PXR (**Fig 6D** and Supplement 17). Conversely, regulators associated with inflammation (e.g. Interferon alpha, TGFB1, IL2 and CD44) were highly activated in all human liver disease conditions. Altogether, the analysis revealed an inflammation-associated suppression of metabolic gene networks in acute and chronic liver injury of human and mouse.

Discussion

Liver damage leads to the activation of numerous signaling and transcriptional regulatory networks, whose functions in tissue injury and regeneration are not fully understood (Forbes et al., 2014). Here, we applied time-resolved transcriptomics of mouse liver after acute intoxication with CCl_4 combined with bioinformatics to unravel the sequential processes during early onset of injury and subsequent regeneration. The most significant biological motifs upon CCl_4 administration are upregulated gene clusters representing stress signaling (i.e. endoplasmic reticulum stress) and inflammation, which is accompanied by downregulation of genes representing mature liver functions particularly endogenous as well as xenobiotic metabolism. This concomitant inflammation/metabolism response peaks between 1 and 24h after CCl_4 intoxication. In contrast, genes associated with proliferation and tissue restoration peak only 48h after intoxication. Analysis of lobular zonation showed that stress signaling is limited to PC hepatocytes; whereas, increased expression of inflammation and reduced expression of metabolism associated genes occurs throughout the liver parenchyma. Thus, suppression of metabolic functions occurs not only in PC hepatocytes that will undergo necrosis upon CCl_4 exposure but also in PP hepatocytes that will survive intoxication. All lobular zones respond already within the first two hours to intoxication, although CCl_4 is metabolically activated to its toxic metabolites, the trichloromethyl and the trichloromethylperoxy radicals, only by approximately 40% of most central hepatocytes of liver lobules, because only these cells express the toxifying enzyme cytochrome P450 2E1 (Godoy et al., 2013).

The significance of suppressing mature liver functions during inflammatory conditions is not fully understood. One possibility is that this response is necessary for efficient regeneration upon acute liver injury. In support, suppressing HNF4 expression in adult mouse liver with a tamoxifen-controlled system decreased multiple genes related to metabolic liver functions, while concomitantly increasing expression of proliferation genes, thus linking HNF4 to hepatocyte proliferation (Bonzo et al., 2012). HNF4 downregulation is also observed in hepatocellular carcinoma (Lazarevich et al., 2004; 2010), and its inhibition leads to epithelial-to-mesenchymal transition in mature hepatocytes and hepatoma cell lines (Santangelo et al., 2011), which may also be

necessary for reestablishment of tissue architecture after massive injuries (Hoehme et al., 2010). Furthermore, only a relatively small fraction of the metabolic capacity of the normal liver is sufficient for survival. Therefore, inflammation-mediated downregulation of metabolic enzymes and mature liver functions will not lead to major pathophysiological consequences. It may, however, support the regeneration process by transiently focusing more resources on proliferation and re-establishment of a functional microarchitecture.

An interesting observation is that Cluster group 2 genes (associated with mature liver functions downregulated after CCl_4) are enriched in PP hepatocytes. This downregulation overlaps with the upregulation or nuclear accumulation of the inflammatory transcription factor CEBPD which not only occurs in Cyp2E1 positive PC, but also expands to most PP hepatocytes. Ingenuity pathway analysis provides support that the same upstream regulators are responsible for both the upregulation of inflammatory genes and the downregulation of genes associated with metabolism and mature liver functions. For example, the most enriched IPA pathway 'LPS/IL-1 mediated inhibition of RXR function' comprises upregulation of the pro-inflammatory signaling factor c-Jun and downregulation of the bile salt export carrier BSEP, a typical function of mature livers (**Fig. 4D**). Similarly, MRP4, a gene known to be upregulated in inflamed and cholestatic livers to export bile acids to blood (Jansen et al., 2017) is increased while CYP7A1, the gene responsible for a key step in bile acid synthesis is downregulated. Further triggers of the coordinated inflammatory response are cytokines, such as TNF, IL5, IL6 and SPP1 and signal transducers, including JUNB, MAPK1, and NFKBIN; however, the underlying mechanisms coupling increased expression of inflammatory genes to reduced expression of genes responsible for mature liver functions remain unknown. Hypotheses, include cytokines released into the circulation that influence the entire liver, signals mediated by cell types sensing damage and releasing inflammatory cytokines, such as LSEC (Ding et al., 2010), or cytokines rapidly diffusing from the PC wound to the non-injured PP tissue.

IPA and GSEA showed high overrepresentation of ER stress pathways throughout early stages of acute liver injury. Recently, it was reported that hepatocyte death by CCl_4 is mediated by the ER adapter stimulator of interferon genes (STING) via interferon regulatory factor 3 (IRF3) (Iracheta-Vellve et al., 2016), suggesting that transient ER

stress may funnel subsequent inflammatory pathways towards hepatocyte death. However, further studies have revealed protective roles for ER stress signaling in liver pathophysiology. For example, we did not observe a reduction in CCl_4-induced liver damage in a knockout mouse model of CHOP, a transcription factor activated in response to ER stress (Campos et al., 2014). Also, hepatocyte-specific deletion of the ER-stress sensor IRE1a resulted in enhanced liver injury by CCl_4 which was associated with dampened STAT3 activation (Liu et al., 2015). Similarly, activated IRE1a protected against acetaminophen hepatotoxicity via the downregulation of Cyp2e1 mRNA due to its RNAse activity (Hur et al., 2012). Furthermore, ER stress can affect the functions of non-parenchymal cells, for example by promoting activation of stellate cells (Kim et al., 2016). Due to this complexity, the pathophysiological consequences of ER-stress are not yet fully understood in the context of liver disease.

The detailed identification of TRNs mediating liver damage and regeneration is fundamental to establish risk, diagnosis and therapeutic intervention. Our findings provide a detailed, time-resolved description of gene networks in mouse liver upon acute injury and regeneration. Coordinated induction of inflammation/cell stress associated genes accompanied by down regulation of metabolic genes are controlled by the same upstream regulators and represent a pattern that occurs similarly in acute and chronic liver diseases in humans and mice.

Figure legends

Fig. 1. Experimental design, principal component and cluster analysis of time-resolved expression data after CCl_4 intoxication. (A) Overview of the experimental setup for acute intoxication with CCl_4. Liver tissue sections were collected at the indicated time points after a single intraperitoneal injection of CCl_4 (1.6 g/kg). N = 5 mice per time point. (B) Principal component analysis of the top 1,000 differentially expressed genes in the combined time series after CCl_4. The different blue tones denote the time points of each biological replica (mouse) for liver tissue after CCl_4 administration. Control liver tissues (day 1 treated with olive oil) are indicated in dark green. (C-F) Published genome-wide data from mouse models used for comparison in the present study. (G) Genome-wide data from human liver tissue used for comparison with the mouse data.

Fig 2. Grouping of time-resolved gene clusters in mouse liver after CCl_4 intoxication. Time-dependent fuzzy clustering was performed with deregulated genes in mouse liver tissue after CCl_4 intoxication. Dots represent mean scaled values of all genes in each cluster. Error bars represent standard deviations. The three cluster groups were formed based on similarities in overrepresented gene ontology (GO), KEGG motifs and pathways identified by Ingenuity Pathway Analysis (IPA). The figure shows the most significantly enriched GO and KEGG annotations, and representative deregulated genes for each cluster. Representative transcription factors (TF) include the strongest deregulated genes with known function as transcriptional regulator identified in each cluster. The representative transcription factor binding sites and representative pathways (IPA) correspond to those with highest statistical significance ($p<10^{-5}$).

Fig. 3. Spatiotemporal zonation of signaling and gene expression during CCl_4 intoxication. (A) Immunostaining analysis of c-Jun, CEBPD and HNF4 during acute liver injury. Control tissues correspond to mouse liver on day 1 after injection of vehicle (olive oil). Representative of at least three biological replicas per time point and condition. (B) Venn diagrams showing overlap between PP or PC-enriched genes and the three CCl_4-cluster groups. Red and blue circles represent PP or PC genes, respectively. Dark green

circles represent genes contained in each CCl_4-cluster (C-D). Western blot analysis of whole liver extracts after CCl_4 intoxication. Blots are representative from at least three biological replicas.

Fig. 4. Inflammation and ER-stress dependent suppression of metabolism-associated genes. (A) Graphical representation of all differential genes after CCl_4 intoxication. Dots represent mean scaled values of all genes at each time point. Light red and blue areas represent standard deviation. (B-C) Heatmap representation of the top 40 canonical pathways (B) and upstream regulators (C) significantly altered during CCl_4 intoxication. (D) Heatmap representation of the top 10 up and downregulated genes in the two strongest overrepresented pathways identified by IPA. (E) Overlap between downregulated genes after LPS or tunicamycin administration, and after CCl_4 intoxication (i.e. genes in Cluster group 3). Both overlaps were highly significant ($<10^{-5}$). (F) Selected overrepresented GO and KEGG terms in the overlapped genes from (E).

Fig. 5. Identification of inflammation-dependent suppression of liver metabolism gene networks in experimental HCC. (A) Spearman correlation analysis between differentially expressed genes in HCC vs acute intoxication with CCl_4 (2h to day 16). (B) Venn diagrams showing overlap between upregulated or downregulated genes at the two time points of highest correlation (days 1 and 2) between acute CCl_4 intoxication and HCC. All overlaps are highly significant ($p<0.001$). (C-D) Heatmap representation of the top 40 canonical pathways (C) or activated/inactivated upstream regulators (D) identified as significantly altered by IPA in HCC and in acute CCl_4 intoxication.

Fig. 6. Identification of an inflammation-dependent suppression of liver metabolism gene networks in human liver disease. A) Heatmap representation of the top 30 canonical pathways identified as significantly altered by IPA in nonalcoholic fatty liver disease (score 0-1; 3-4), hepatitis B infected liver (HBV) and hepatocellular carcinoma (HCC). (B-C) Heatmap representation of the top 10 up and downregulated genes in the pathways ‘FXR/RXR activation’ and ‘LPS/IL-1 mediated inhibition of RXR function’

identified by IPA. (D) Heatmap representation of the top 30 upstream regulators identified as significantly activated or deactivated by IPA in human liver disease.

References

[1] Karin M, Clevers H. Reparative inflammation takes charge of tissue regeneration. Nature 2016;529:307-315.

[2] Campos G, Schmidt-Heck W, Ghallab A, Rochlitz K, Putter L, Medinas DB, et al. The transcription factor CHOP, a central component of the transcriptional regulatory network induced upon CCl4 intoxication in mouse liver, is not a critical mediator of hepatotoxicity. Archives of toxicology 2014;88:1267-1280.

[3] Michalopoulos GK. Principles of liver regeneration and growth homeostasis. Comprehensive Physiology 2013;3:485-513.

[4] Rashid HO, Yadav RK, Kim HR, Chae HJ. ER stress: Autophagy induction, inhibition and selection. Autophagy 2015;11:1956-1977.

[5] Hart LS, Cunningham JT, Datta T, Dey S, Tameire F, Lehman SL, et al. ER stress-mediated autophagy promotes Myc-dependent transformation and tumor growth. The Journal of clinical investigation 2012;122:4621-4634.

[6] Braeuning A, Ittrich C, Kohle C, Hailfinger S, Bonin M, Buchmann A, et al. Differential gene expression in periportal and perivenous mouse hepatocytes. The FEBS journal 2006;273:5051-5061.

[7] Godoy P, Schmidt-Heck W, Natarajan K, Lucendo-Villarin B, Szkolnicka D, Asplund A, et al. Gene networks and transcription factor motifs defining the differentiation of stem cells into hepatocyte-like cells. Journal of hepatology 2015;63:934-942.

[8] Moylan CA, Pang H, Dellinger A, Suzuki A, Garrett ME, Guy CD, et al. Hepatic gene expression profiles differentiate presymptomatic patients with mild versus severe nonalcoholic fatty liver disease. Hepatology 2014;59:471-482.

[9] Farci P, Diaz G, Chen Z, Govindarajan S, Tice A, Agulto L, et al. B cell gene signature with massive intrahepatic production of antibodies to hepatitis B core antigen in hepatitis B virus-associated acute liver failure. Proceedings of the National Academy of Sciences of the United States of America 2010;107:8766-8771.

[10] Arai M, Yokosuka O, Chiba T, Imazeki F, Kato M, Hashida J, et al. Gene expression profiling reveals the mechanism and pathophysiology of mouse liver regeneration. The Journal of biological chemistry 2003;278:29813-29818.

[11] Forbes SJ, Rosenthal N. Preparing the ground for tissue regeneration: from mechanism to therapy. Nature medicine 2014;20:857-869.

[12] Forbes SJ, Newsome PN. Liver regeneration - mechanisms and models to clinical application. Nature reviews Gastroenterology & hepatology 2016;13:473-485.

[13] Young MB, DiSilvestro MR, Sendera TJ, Freund J, Kriete A, Magnuson SR. Analysis of gene expression in carbon tetrachloride-treated rat livers using a novel bioarray technology. The pharmacogenomics journal 2003;3:41-52.

[14] Chung H, Hong DP, Jung JY, Kim HJ, Jang KS, Sheen YY, et al. Comprehensive analysis of differential gene expression profiles on carbon tetrachloride-induced rat liver injury and regeneration. Toxicology and applied pharmacology 2005;206:27-42.

[15] Zidek N, Hellmann J, Kramer PJ, Hewitt PG. Acute hepatotoxicity: a predictive model based on focused illumina microarrays. Toxicological sciences : an official journal of the Society of Toxicology 2007;99:289-302.

[16] White P, Brestelli JE, Kaestner KH, Greenbaum LE. Identification of transcriptional networks during liver regeneration. The Journal of biological chemistry 2005;280:3715-3722.
[17] Wang B, Cai SR, Gao C, Sladek FM, Ponder KP. Lipopolysaccharide results in a marked decrease in hepatocyte nuclear factor 4 alpha in rat liver. Hepatology 2001;34:979-989.
[18] Dubois-Pot-Schneider H, Fekir K, Coulouarn C, Glaise D, Aninat C, Jarnouen K, et al. Inflammatory cytokines promote the retrodifferentiation of tumor-derived hepatocyte-like cells to progenitor cells. Hepatology 2014;60:2077-2090.
[19] Ogata M, Hino S, Saito A, Morikawa K, Kondo S, Kanemoto S, et al. Autophagy is activated for cell survival after endoplasmic reticulum stress. Molecular and cellular biology 2006;26:9220-9231.
[20] Bonzo JA, Ferry CH, Matsubara T, Kim JH, Gonzalez FJ. Suppression of hepatocyte proliferation by hepatocyte nuclear factor 4alpha in adult mice. The Journal of biological chemistry 2012;287:7345-7356.
[21] Lazarevich NL, Cheremnova OA, Varga EV, Ovchinnikov DA, Kudrjavtseva EI, Morozova OV, et al. Progression of HCC in mice is associated with a downregulation in the expression of hepatocyte nuclear factors. Hepatology 2004;39:1038-1047.
[22] Lazarevich NL, Shavochkina DA, Fleishman DI, Kustova IF, Morozova OV, Chuchuev ES, et al. Deregulation of hepatocyte nuclear factor 4 (HNF4)as a marker of epithelial tumors progression. Experimental oncology 2010;32:167-171.
[23] Santangelo L, Marchetti A, Cicchini C, Conigliaro A, Conti B, Mancone C, et al. The stable repression of mesenchymal program is required for hepatocyte identity: a novel role for hepatocyte nuclear factor 4alpha. Hepatology 2011;53:2063-2074.
[24] Hoehme S, Brulport M, Bauer A, Bedawy E, Schormann W, Hermes M, et al. Prediction and validation of cell alignment along microvessels as order principle to restore tissue architecture in liver regeneration. Proceedings of the National Academy of Sciences of the United States of America 2010;107:10371-10376.
[25] Ding BS, Nolan DJ, Butler JM, James D, Babazadeh AO, Rosenwaks Z, et al. Inductive angiocrine signals from sinusoidal endothelium are required for liver regeneration. Nature 2010;468:310-315.
[26] Iracheta-Vellve A, Petrasek J, Gyongyosi B, Satishchandran A, Lowe P, Kodys K, et al. Endoplasmic Reticulum Stress-induced Hepatocellular Death Pathways Mediate Liver Injury and Fibrosis via Stimulator of Interferon Genes. The Journal of biological chemistry 2016;291:26794-26805.
[27] Liu Y, Shao M, Wu Y, Yan C, Jiang S, Liu J, et al. Role for the endoplasmic reticulum stress sensor IRE1alpha in liver regenerative responses. Journal of hepatology 2015;62:590-598.
[28] Hur KY, So JS, Ruda V, Frank-Kamenetsky M, Fitzgerald K, Koteliansky V, et al. IRE1alpha activation protects mice against acetaminophen-induced hepatotoxicity. The Journal of experimental medicine 2012;209:307-318.
[29] Kim RS, Hasegawa D, Goossens N, Tsuchida T, Athwal V, Sun X, et al. The XBP1 Arm of the Unfolded Protein Response Induces Fibrogenic Activity in Hepatic Stellate Cells Through Autophagy. Scientific reports 2016;6:39342.

Godoy P, Hewitt NJ, Albrecht U, et al., Recent advances in 2D and 3D in vitro systems using primary hepatocytes, alternative hepatocyte sources and non-parenchymal liver cells and their use in investigating mechanisms of hepatotoxicity, cell signaling and ADME. Arch Toxicol. 2013 Aug;87(8):1315-530. doi: 10.1007/s00204-013-1078-5.

Jansen PL, Ghallab A, Vartak N, Reif R, Schaap FG, Hampe J, Hengstler JG. The ascending pathophysiology of cholestatic liver disease. Hepatology. 2017 Feb;65(2):722-738. doi: 10.1002/hep.28965.

Figure

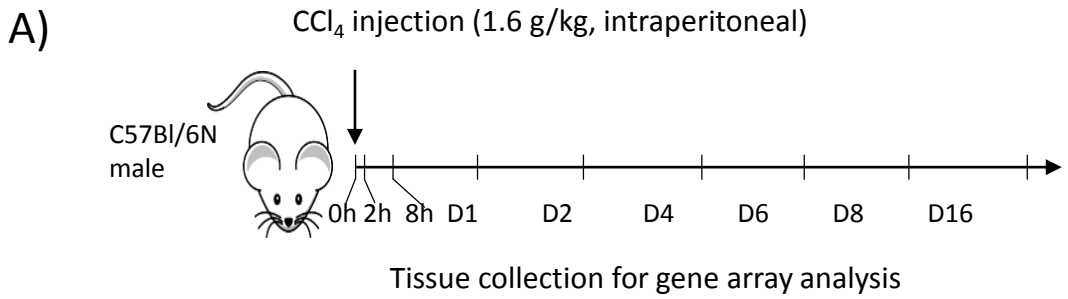
A)
CCl_4 injection (1.6 g/kg, intraperitoneal)
C57Bl/6N
male
0h 2h 8h D1 D2 D4 D6 D8 D16
Tissue collection for gene array analysis

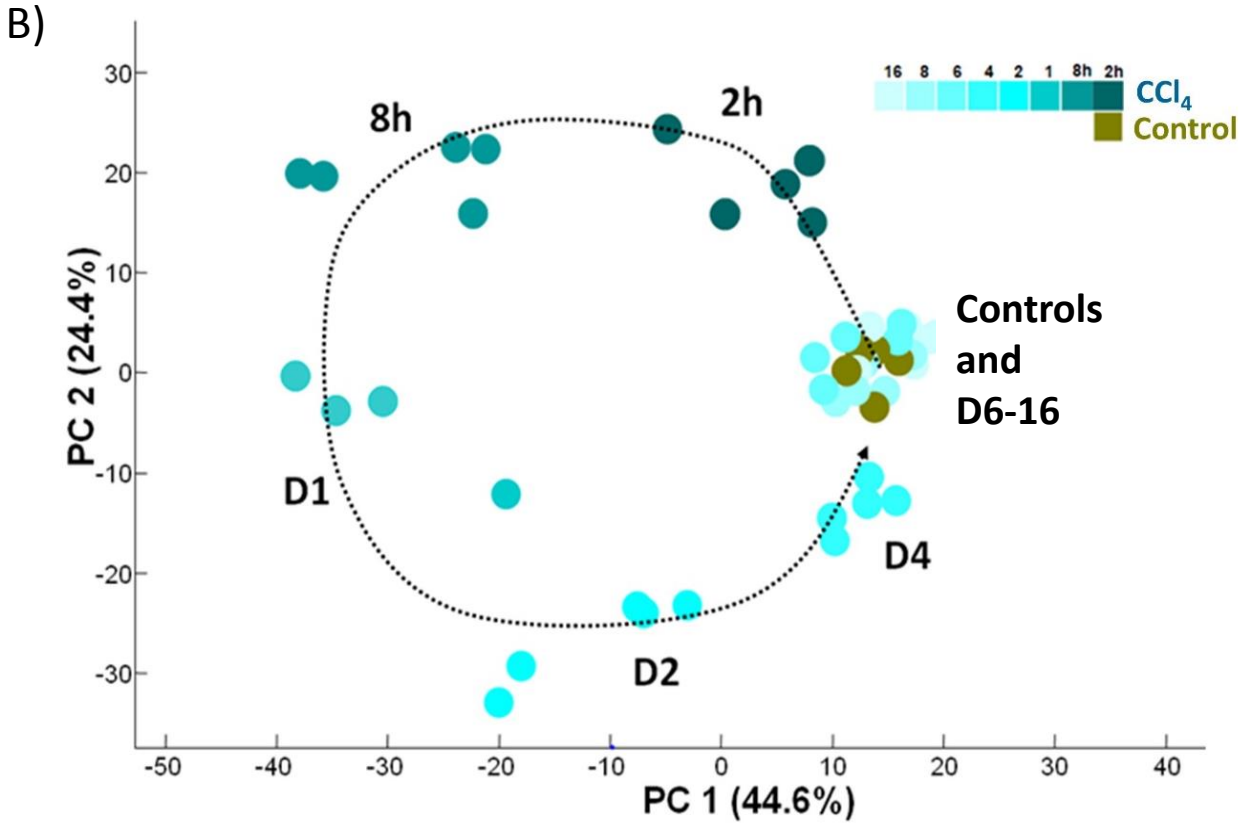
B)
16 8 6 4 2 1 8h 2h
CCl_4
Control
8h
2h
D1
D2
D4
Controls
and
D6-16
PC 2 (24.4%)
PC 1 (44.6%)
30
20
10
0
-10
-20
-30
-50
-40
-30
-20
-10
0
10
20
30
40

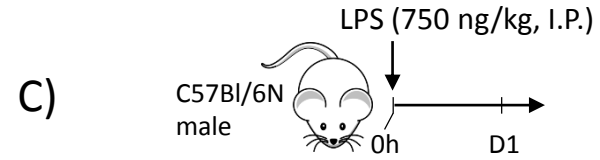
C)
LPS (750 ng/kg, I.P.)
C57Bl/6N
male
0h
D1

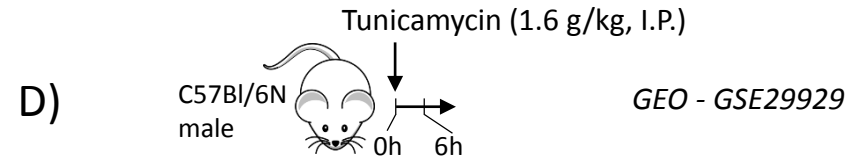
D)
Tunicamycin (1.6 g/kg, I.P.)
C57Bl/6N
male
0h
6h
GEO - GSE29929

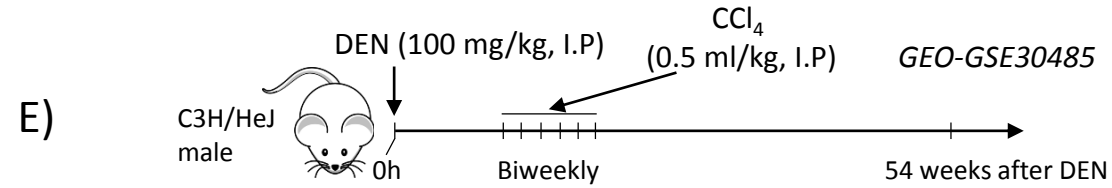
E)
DEN (100 mg/kg, I.P)
CCl_4
(0.5 ml/kg, I.P)
GEO-GSE30485
C3H/HeJ
male
0h
Biweekly
54 weeks after DEN

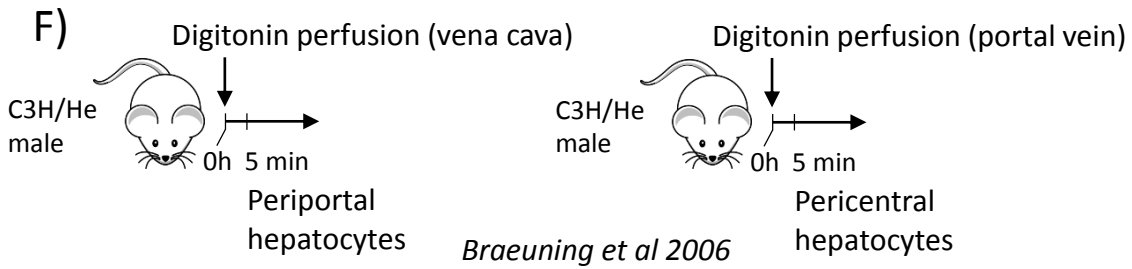
F)
Digitonin perfusion (vena cava)
C3H/He
male
0h 5 min
Periportal
hepatocytes
Digitonin perfusion (portal vein)
C3H/He
male
0h 5 min
Pericentral
hepatocytes
Braeuning et al 2006

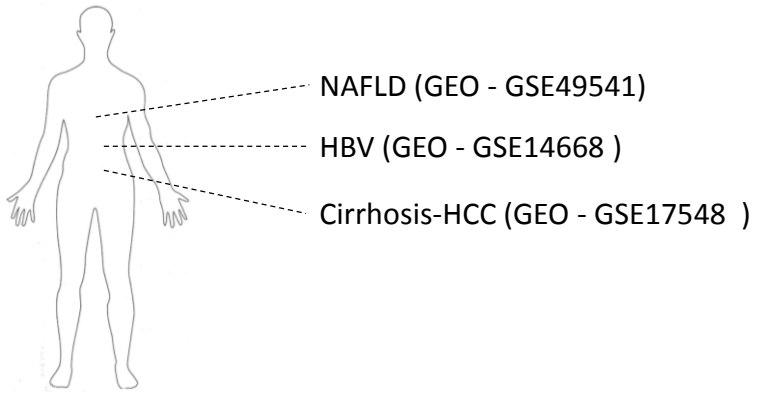
G)
NAFLD (GEO - GSE49541)
HBV (GEO - GSE14668)
Cirrhosis-HCC (GEO - GSE17548)

Fig. 1

Figure

			Biological motifs			Regulatory networks		
			Overrepresented motifs (GO)	**Overrepresented Pathways (KEGG)**	**Representative genes**	**Representative deregulated TF**	**Representative TFBS**	**Representative upstream regulators (IPA)**
Cluster group 1 Cell stress, UPR, Inflammation	Cluster 1a (205 genes)	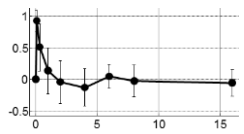	**RNA metabolism, Regulation of transcription, Response to stress, Regulation of kinase activity, Programmed cell death,** Cell cycle, Response to ER stress	**MAPK signaling pathway,** TNF signaling pathway	Gadd45a, Gadd45g, Btg2, Dusp6, Fgf21, Trp53inp1, Ppp1r15a, Bcl3, Cxcl1	Jun, Fos, Junb, Cebpb, Cebpd, Atf3, Egr1, Id3, Ddit4, **Klf10**, Maff, Ier2	**E2F, Sp1, ZF5, HIC1, ATF,** ATF4, AHRHIF, AP-2, EGR, ZFN219, Tax/CREB, MAZ	IRIF2AK3(PERK), NUPR1, ATM, ELK3, ATF4, FOXO1, IKBKB, MAPK9, FOXO3, AK, CREM, IL1B, CREB1, TNF, p38, E NFATC3, NR1I3(CAR), EGR1, CEBPB, STAT, EGF, JUN, HGF
	Cluster 1b (510 genes)	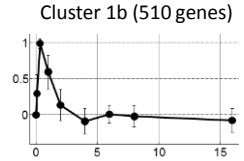	**Ribosome biogenesis, ER-stress, ERAD pathway; Regulation of gene expression**	**Protein processing in ER, Ribosome biogenesis in eukaryotes,** RNA transport, Epstein-Barr virus infection, Proteasome	Mt2, Sqstm1, Bcl10, Arl4a, Srxn1, Dnajb9, Hsph1, Serpina7, Trib3, Ifrd1	Atf4, Myc, Snai2, Ddit3, Ets2, Klf6, Gata6, Zfand2a, Nfxl1	**ETF, Elk-1, E2F, HIF-1, ATF, Ahr,** GABP, ZF5, c-Myc:Max, AHRHIF, Nrf-1, FOXP1, AP-2	XBP1, EIF2AK3(PERK), ERN1(IRE1a), MYC, CLOCK, CREB1
	Cluster 1c (551 genes)	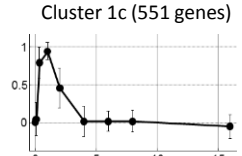	**RNA processing, Regulation of telomerase RNA localization to Cajal body, Nitrogen compound metabolic process, Protein location to ER, Protein folding**	**Protein processin in ER, Protein transport, RNA transport,** Pyrimidine metabolism, Proteasome	Psat1, Ero1l, Nucb2, Cct4, Cct5, Psph, Arf6, Nupr1, P4ha2, Cd14, Lcn2, Ly96, Ccl2, Tnfrsf12a	Ybx3, Ier3, Sox9, Cdkn1a, Yy2, Zfp52	**ETF, Elk-1, E2F, GABP, Sp1, HIF-1, ZF5, AHRHIF, ATF, Nrf-1, AP-2,** E2F-1, Tel-2, Ahr	XBP1, ERN1(IRE1a), NFE2L2(Nrf2), ATF4, EIF2AK3(PERK), HSF2, IL4, ELK1, MYC, ATF6, TRIB3
	Cluster 1d (488 genes)	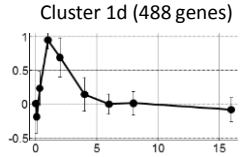	**Protein metabolic process, Response to stress, Translation,** Phagocytosis, Cytoskeleton organization, Cell death	**Protein processing in ER,** Salmonella infection, N-Glycan biosynthesis	Cpe, Xpo1, Macro, Lgals3, Cd68, Ly6d, Ccl6, Camk1, Mmp13, Fgl1, Bax, Ddx39	Ralb, Atf5, Id1	**ETF, Elk-1, Sp1, HIF-1, AHRHIF,** E2F, ZF5, c-Myc:Max, E2F-1, Nrf-1, AP-2, Pax-5, Ahr:Arnt	TP53, XBP1, SRF, CCL5, MLK1-2, TNFSF12, FOS, ERBB2, NR3C1(CAR), NFE2L2(Nrf2), IL6, TGFB1, MYC, HGF, TP73, CXCL12, TNF
Cluster group 2 Metabolism	Cluster 2a (625 genes)	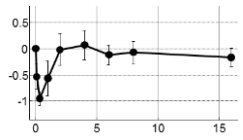	**Metabolic process: Small molecule, Organic acid, Fatty acid, Sterol biosynthesis**	**Steroid biosynthesis,** Chemical carcinogenesis, Drug metabolism-cytochrome p450, Fatty acid degradation	Aldh1b1, Hmgcs1, Adh4, Enpp3, Bdh1, Acat2, Srebf1	Nr0b2(SHP), Nfib, Nr2f6, Nr2f2, Nr5a2, Esr1	**Sp1,** HNF4, LEF1TCF1	**PPARA**, SREBF2, SREBF1, HNF1A, POU2F1, LEP, HNF4A, NR1I2(PXR), MAP4K4, TCF7L2, PPARG
	Cluster 2b (725 genes)	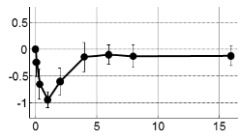	**Metabolic process: Carboxylic acid, Fatty acid, Steroid, Xenobiotic**	**Valine, leucine and isoleucine degradation, Steroid hormone biosynthesis, Peroxisome; Bile secretion, Drug metabolism-cytochrome p450, Fatty acid degradation, PPAR signaling pathway**	Acsm5, Ugt2b1, Abat, Oat, Pck1, Cyp2e1, Car3, Cyp7a1, Cyp8b1, Glul, Cyp2f2, Sult5a1	Nr1h4(FXR), Klf1, Zfp871, Klf15, Foxn3, Nr1i2(PXR), Nr1d1, Dbp, Mafb, Cebpa, Foxo3, Nr1i3(CAR)	**HNF4**, HNF1, GCNF	PPARA , RORA, HNF1, RORC, NR1I2(PXR), HNF4A, **ZBTB20**, NR1H4(FXR), NR0B2(SHP), PPARG, MAP4K4, CNTTB1, RXRA, AHR, PPARD, KLF15, TNF
Cluster group 3 Wound healing, inflammation	Cluster 3a (276 genes)	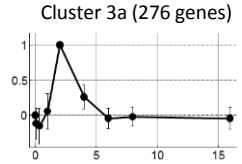	**Cell cycle, Mitotic cell cycle, Nuclear division**	**DNA replication, Mismatch repair, p53 pathway, Pyrimidine metabolism**	Hells, Mcm4, Top2a, Birc5, Cdc20, Ccnb2, Cdk1, Aurka, Mad2l1	Ect2, Nfe2l2(Nrf2), Zfp54, E2f8, Tfdp1, Ikbip	**NF-Y, E2F-1, E2F,** ZF5, Nrf-1, FOXP1	E2F4, CSF2, TP53, CCND1, E2F1, CDK4, NUPR1, FOXM1, E2F6, CDKN1, RARA, TGFB1, YAP1, RB1, AHR, MET, AURKB
	Cluster 3b (248 genes)	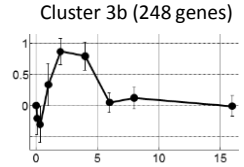	**Immune response, Cell migration, Leukocyte activation, T-cell proliferation, Innate immune response, Phagocytosis, TNF production, ECM organization**	**Lysosome, Staphylococcus aureus infection,** Phagosome, Tuberculosis, ECM-receptor interaction	Coro1, Smoc2, Itgb2, Spp1, Lyz2, Vim, Col1a2, Ly6a, Cd48, Tlr1, Lgals1, Ly6e, Tgfbi, Ly86	Zeb2, Tcf21	AML-1a, PEA3, Osf2	IFNG, TP53, IL13, MYC, TGFB1, STAT6, CTNNB1, TNF, TRIM24, TP73, FGF2, CHUK (IKK1), IKBK, TWIST2, STAT1

Figure

A)

c-Jun

CEBPD

HNF4

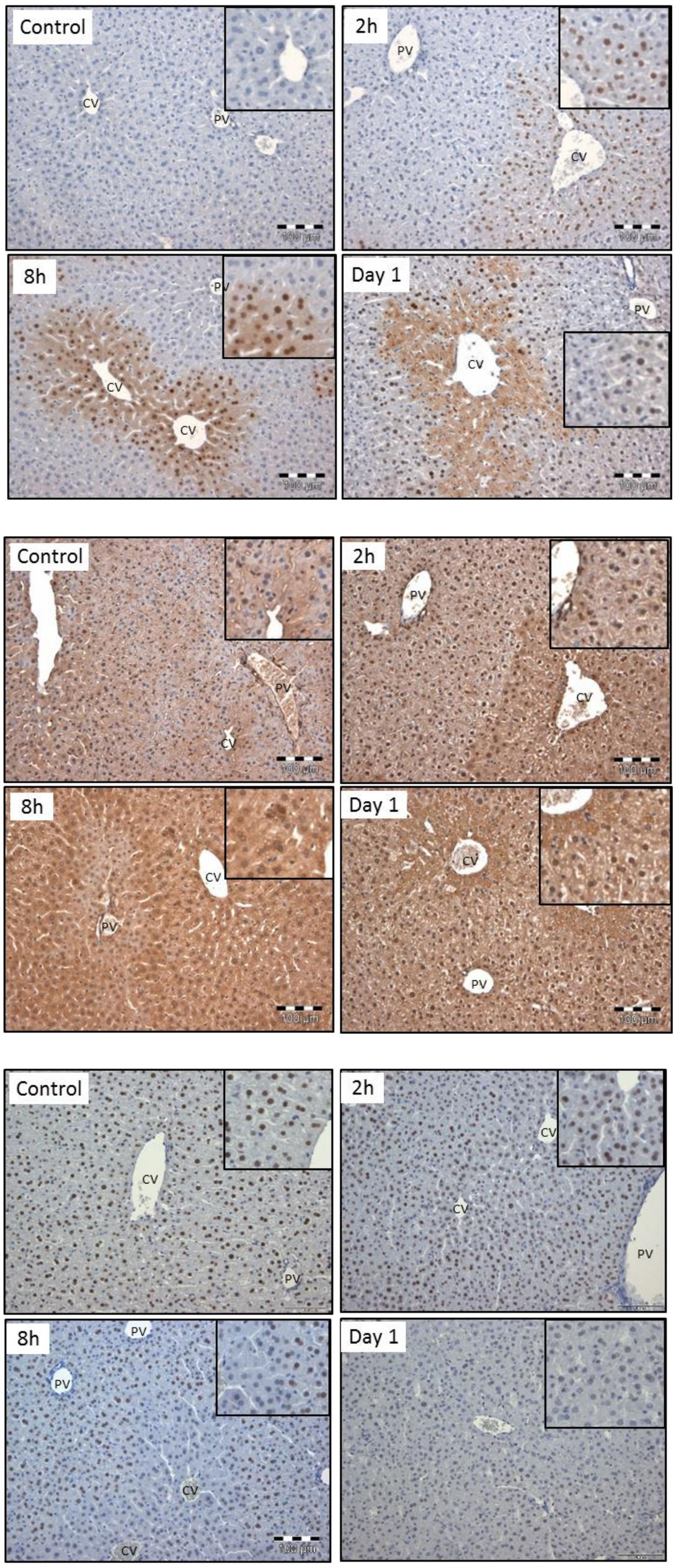

B)

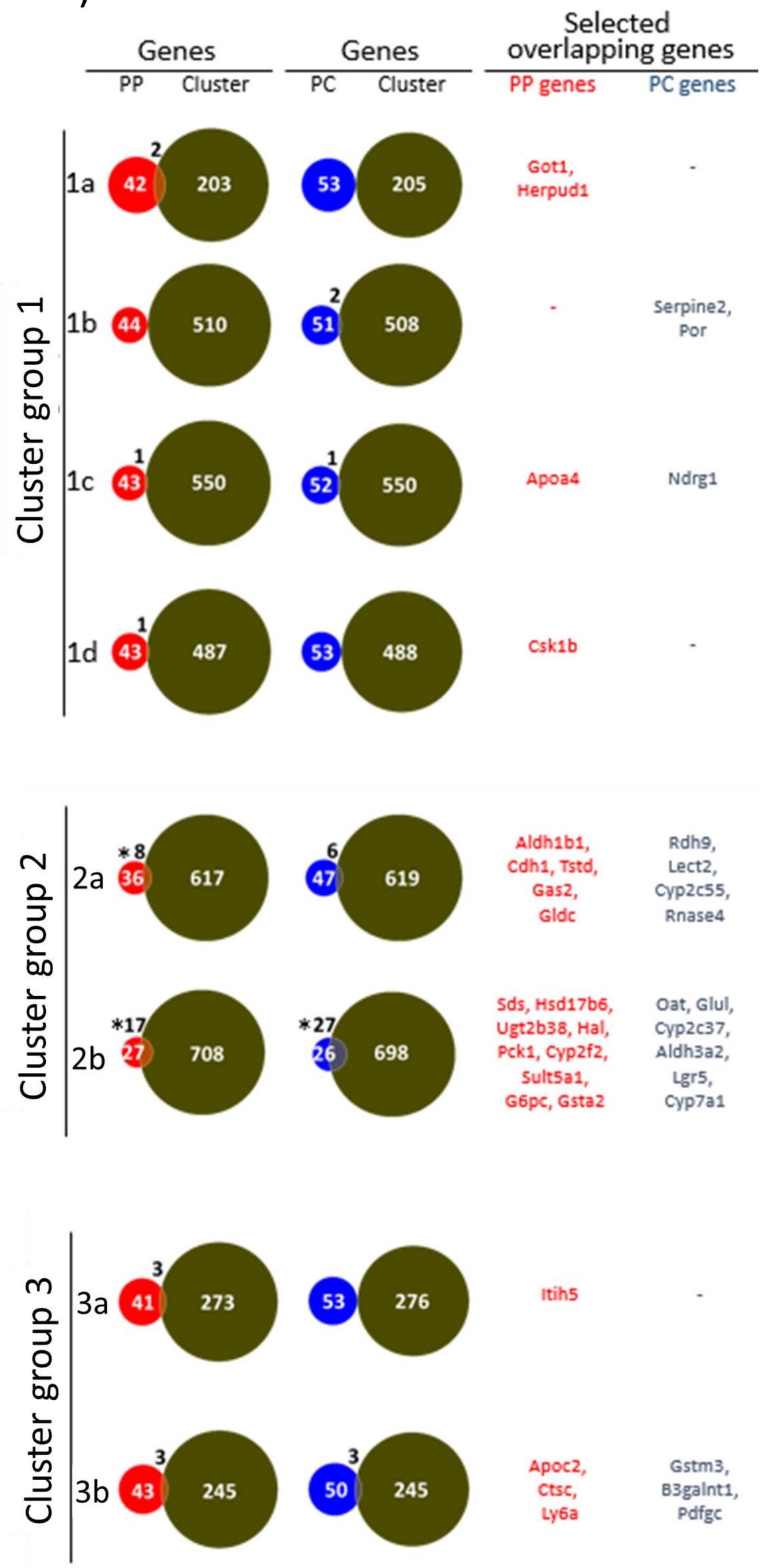

(*= $p<10^{-5}$)

C)

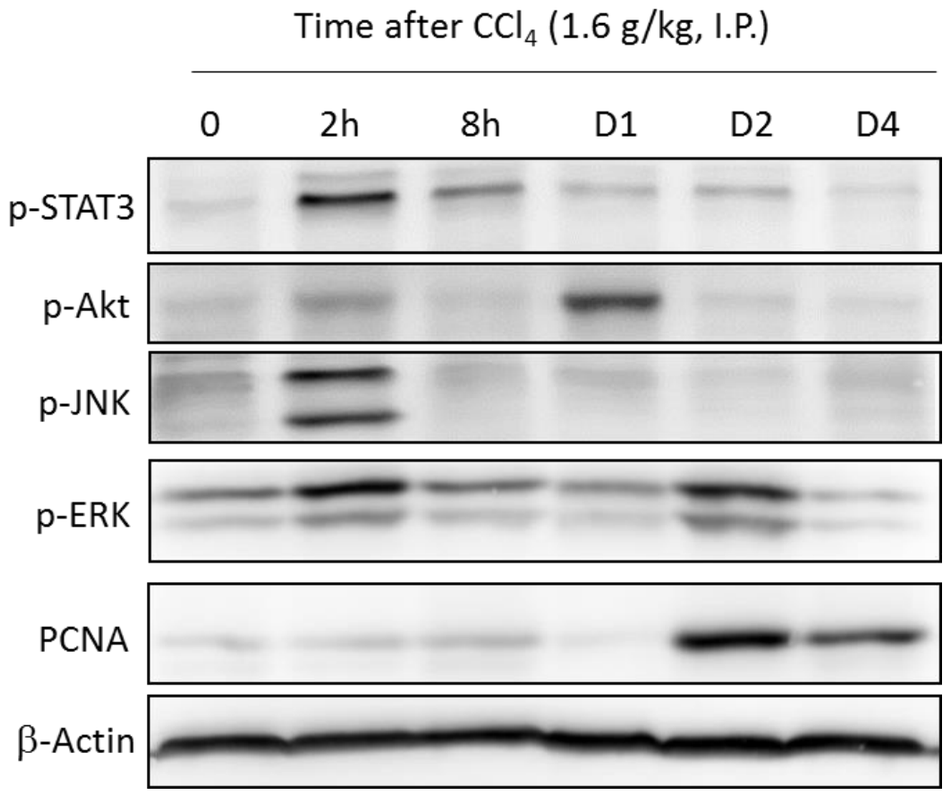

D)

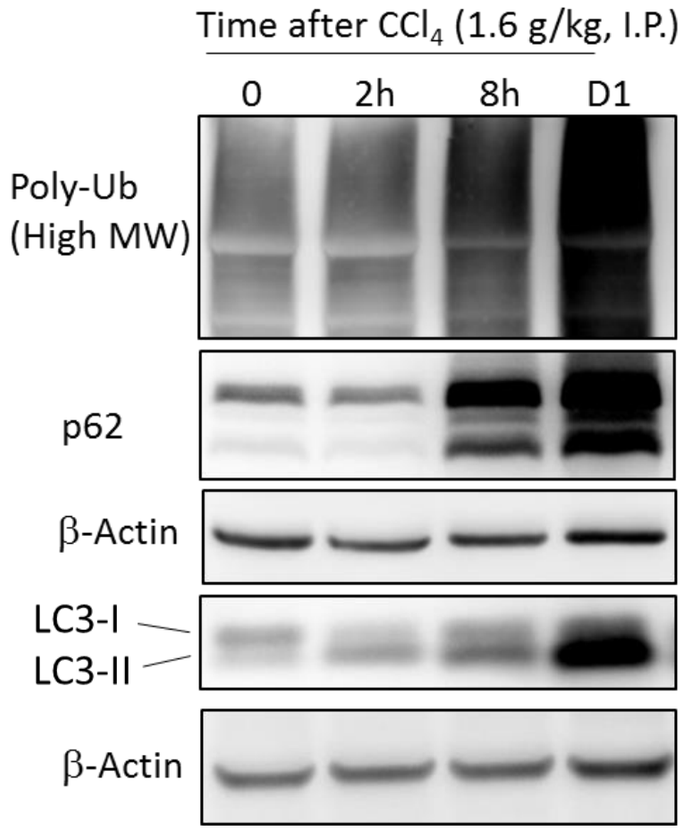

Figure

A)

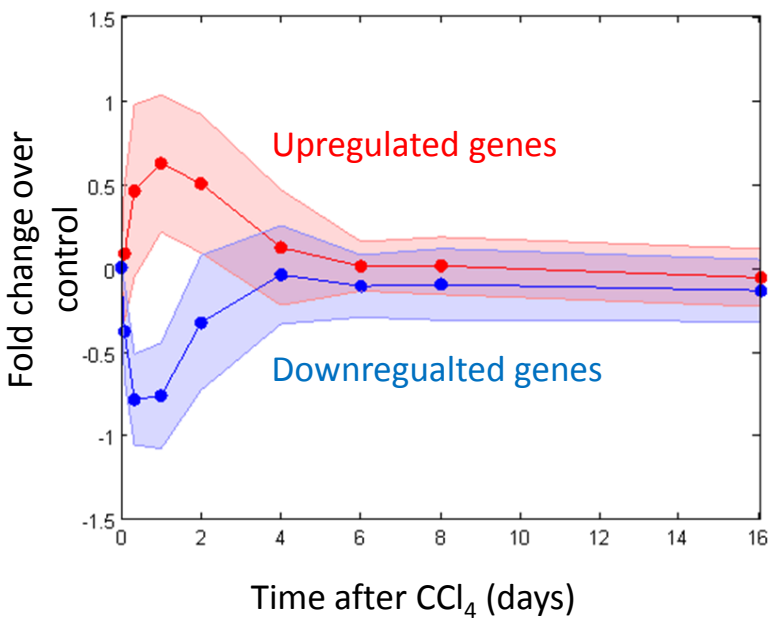

B)

Canonical pathways (IPA)

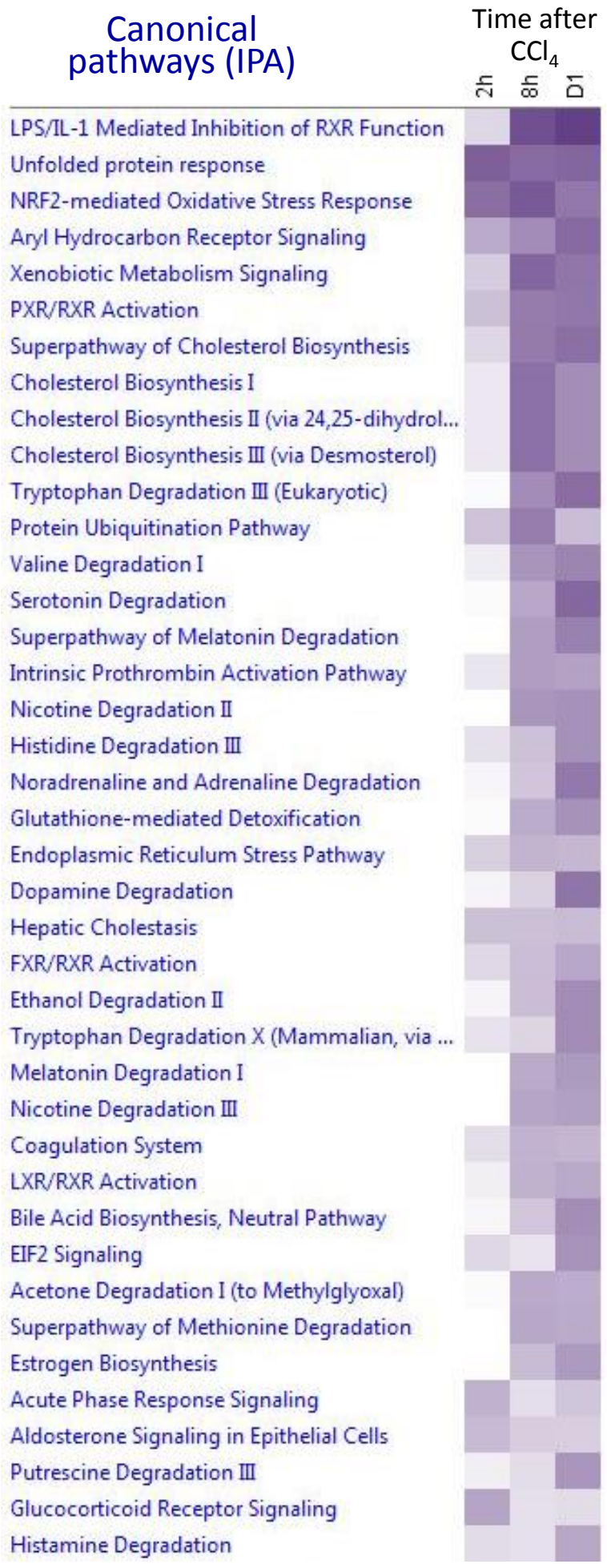

C)

Upstream regulators (IPA)

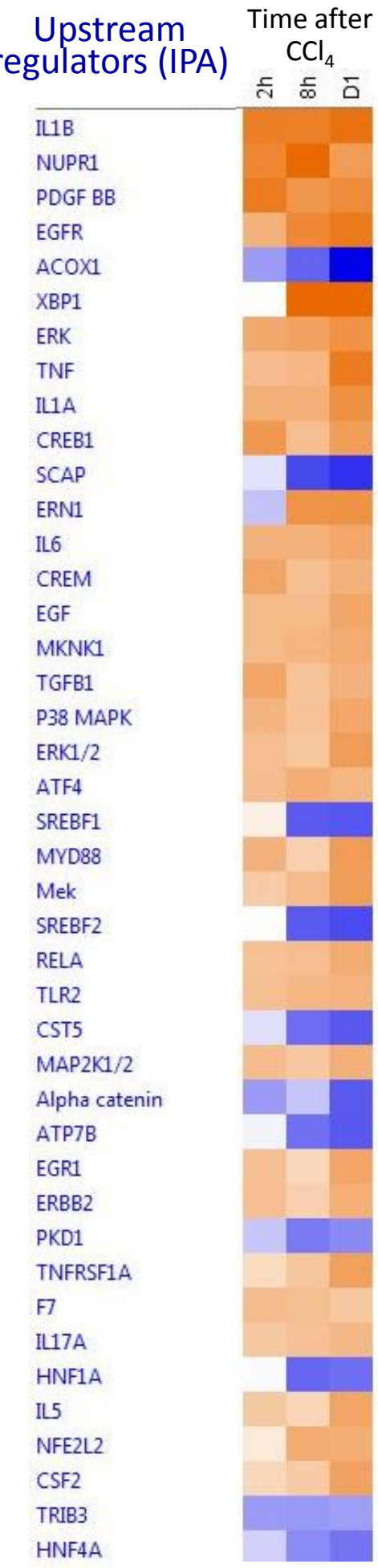

D)

Top 10 up and downregulated genes

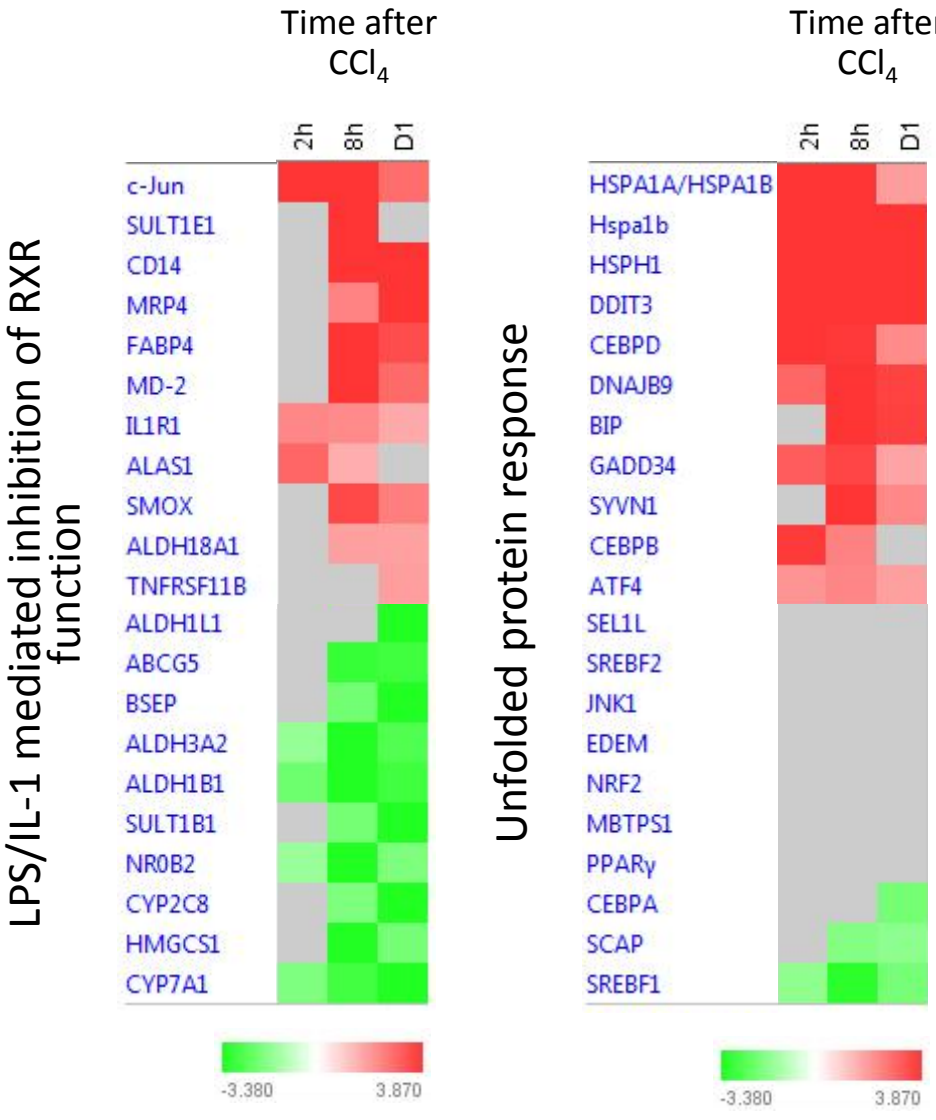

E)

Overlap in downregulated genes

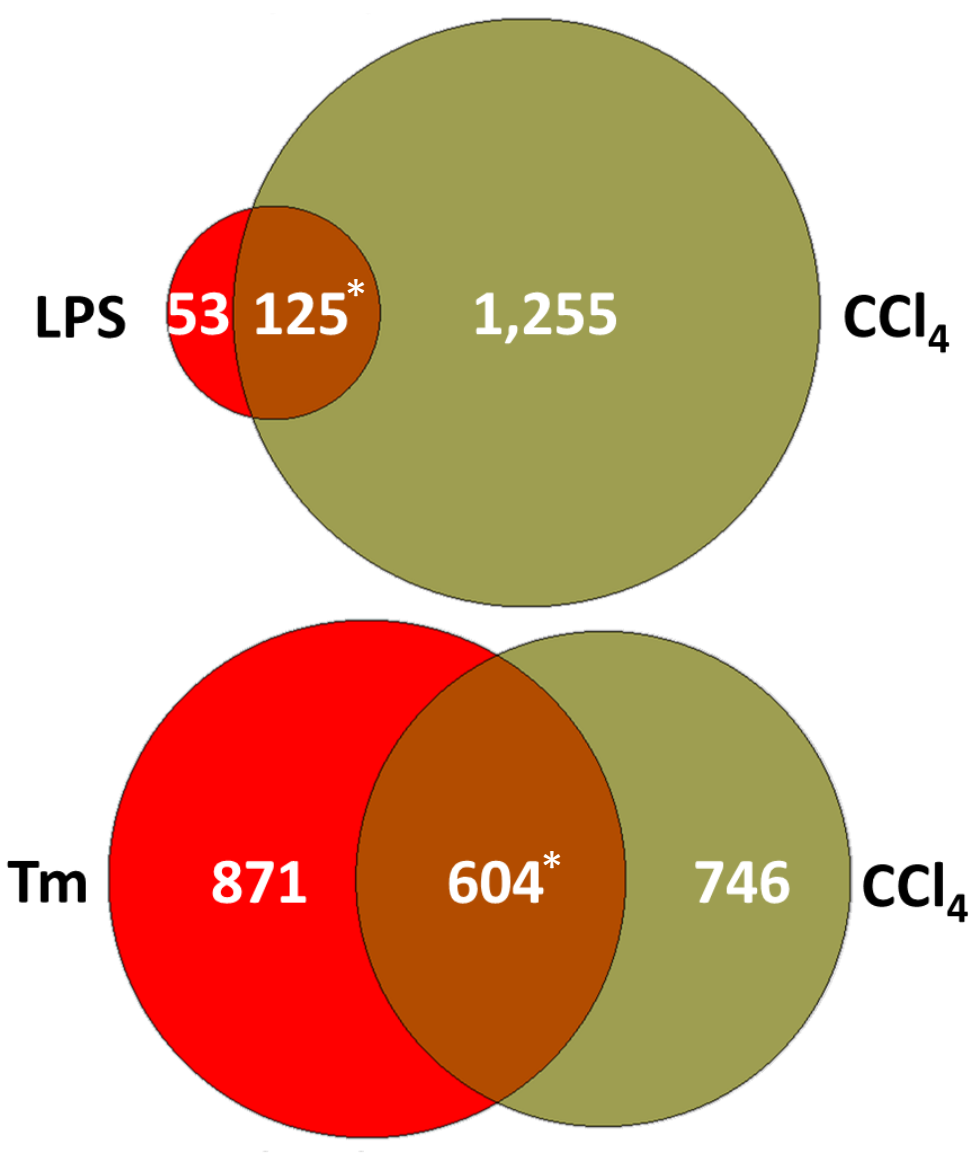

(*=$p<10^{-5}$)

F)

GSEA in overlapped downregulated genes

GO-BP	p-value (LPS/CCl_4)	p-value (Tm/CCl_4)
Small molecule metabolic process	2.24E-32	5.15E-76
Fatty acid metabolic process	1.03E-32	1.98E-27
Steroid metabolic process	7.88E-11	4.40E-20
Xenobiotic metabolic process	6.52E-09	4.47E-06

KEGG	p-value (LPS/CCl_4)	p-value (Tm/CCl_4)
Drug metabolism – cytochrome p450	2.35E-13	4.17E-07
Fatty acid metabolism	1.43E-12	2.71E-12
PPAR signaling pathway	3.88E-09	2.23E-07
ABC transporters	1.23E-05	2.53E-07

Figure

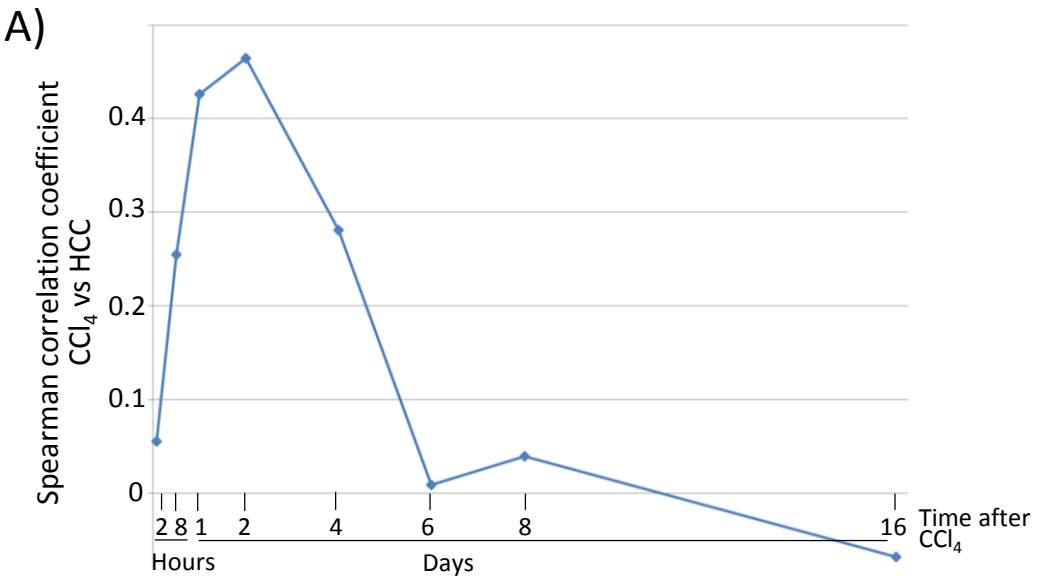
A)
Spearman correlation coefficient
CCl4 vs HCC
0.4
0.3
0.2
0.1
0
2 8 1 2 4 6 8 16
Hours
Days
Time after CCl4

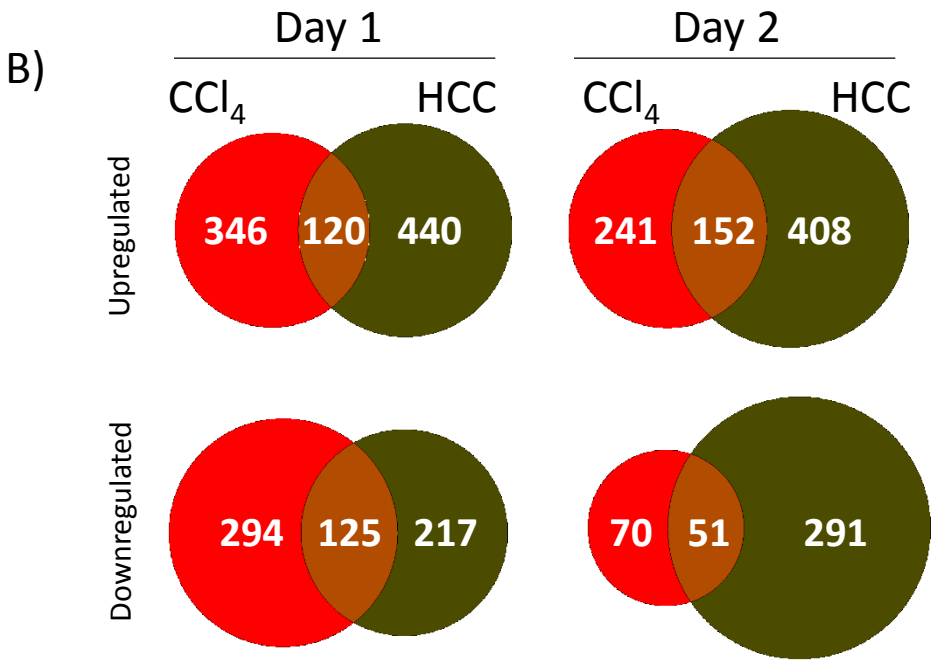
B)
Day 1
Day 2
CCl4
HCC
Upregulated
Downregulated
346
120
440
241
152
408
294
125
217
70
51
291

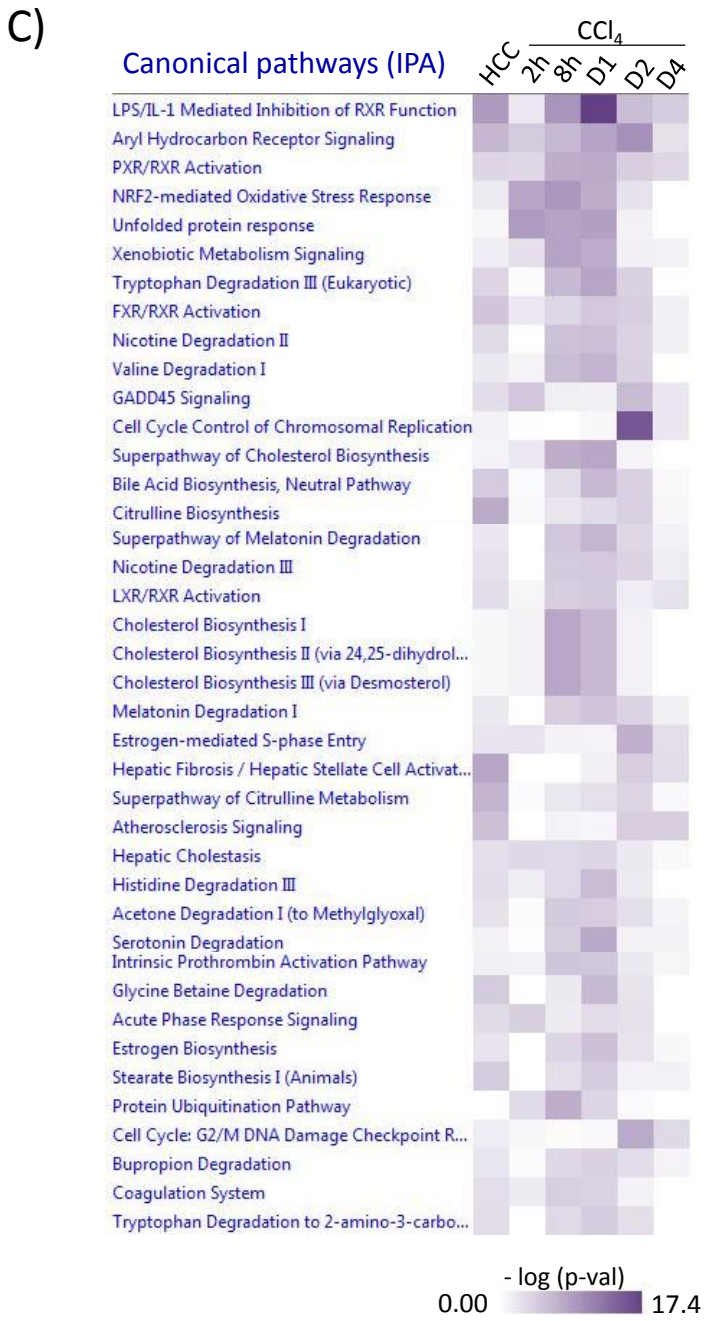
C)
Canonical pathways (IPA)
HCC
CCl4
2h
8h
D1
D2
D4
LPS/IL-1 Mediated Inhibition of RXR Function
Aryl Hydrocarbon Receptor Signaling
PXR/RXR Activation
NRF2-mediated Oxidative Stress Response
Unfolded protein response
Xenobiotic Metabolism Signaling
Tryptophan Degradation III (Eukaryotic)
FXR/RXR Activation
Nicotine Degradation II
Valine Degradation I
GADD45 Signaling
Cell Cycle Control of Chromosomal Replication
Superpathway of Cholesterol Biosynthesis
Bile Acid Biosynthesis, Neutral Pathway
Citrulline Biosynthesis
Superpathway of Melatonin Degradation
Nicotine Degradation III
LXR/RXR Activation
Cholesterol Biosynthesis I
Cholesterol Biosynthesis II (via 24,25-dihydrol...
Cholesterol Biosynthesis III (via Desmosterol)
Melatonin Degradation I
Estrogen-mediated S-phase Entry
Hepatic Fibrosis / Hepatic Stellate Cell Activat...
Superpathway of Citrulline Metabolism
Atherosclerosis Signaling
Hepatic Cholestasis
Histidine Degradation III
Acetone Degradation I (to Methylglyoxal)
Serotonin Degradation
Intrinsic Prothrombin Activation Pathway
Glycine Betaine Degradation
Acute Phase Response Signaling
Estrogen Biosynthesis
Stearate Biosynthesis I (Animals)
Protein Ubiquitination Pathway
Cell Cycle: G2/M DNA Damage Checkpoint R...
Bupropion Degradation
Coagulation System
Tryptophan Degradation to 2-amino-3-carbo...
- log (p-val)
0.00
17.4

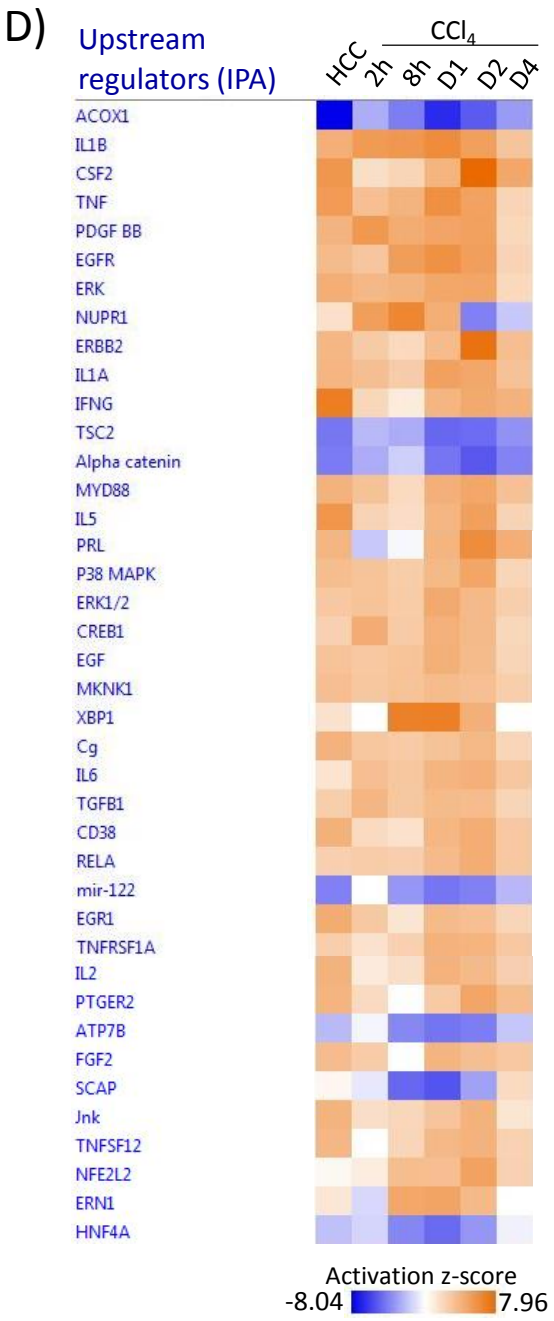
D)
Upstream regulators (IPA)
HCC
CCl4
2h
8h
D1
D2
D4
ACOX1
IL1B
CSF2
TNF
PDGF BB
EGFR
ERK
NUPR1
ERBB2
IL1A
IFNG
TSC2
Alpha catenin
MYD88
IL5
PRL
P38 MAPK
ERK1/2
CREB1
EGF
MKNK1
XBP1
Cg
IL6
TGFB1
CD38
RELA
mir-122
EGR1
TNFRSF1A
IL2
PTGER2
ATP7B
FGF2
SCAP
Jnk
TNFSF12
NFE2L2
ERN1
HNF4A
Activation z-score
-8.04
7.96

Figure

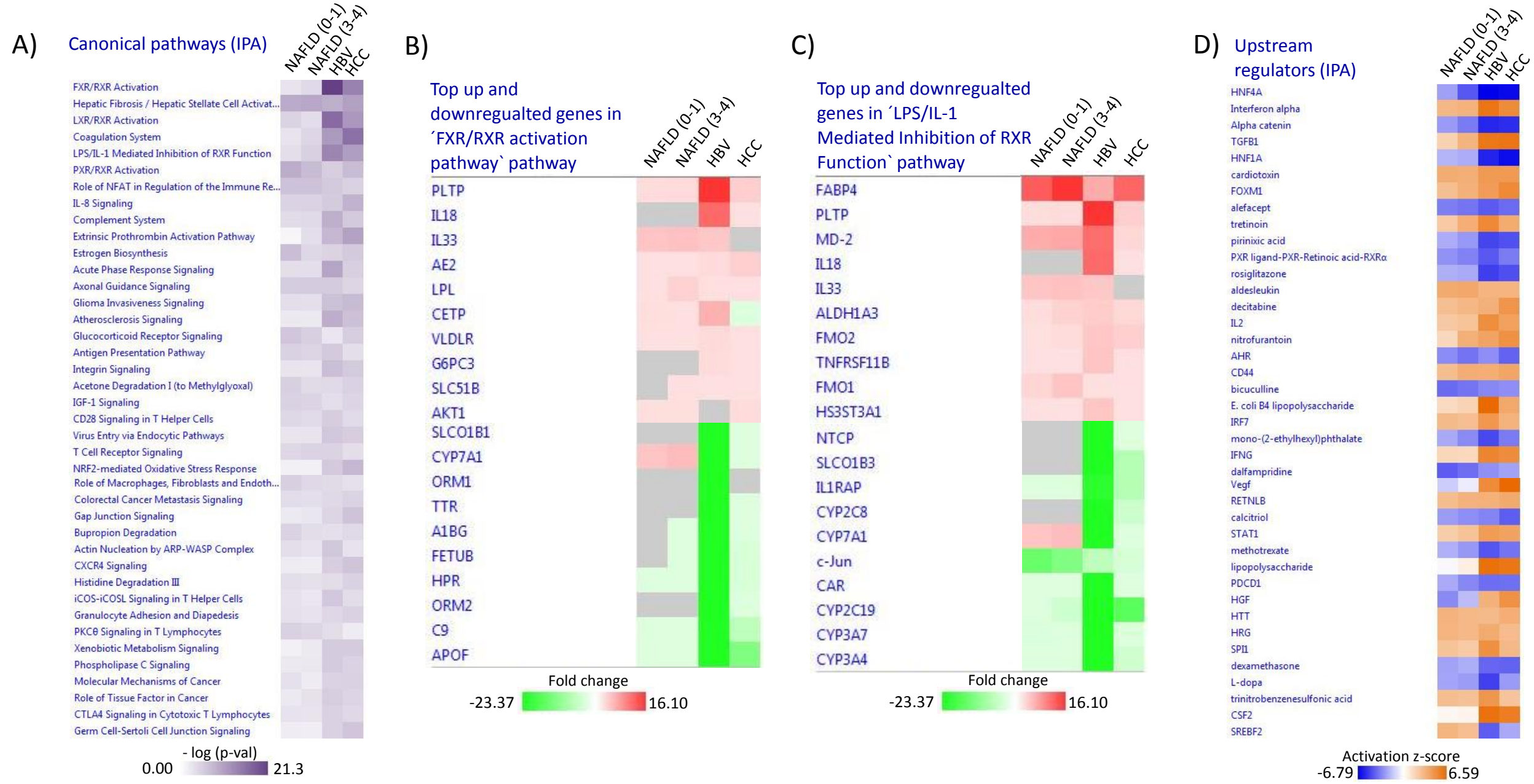
A)
Canonical pathways (IPA)
NAFLD (0-1)
NAFLD (3-4)
HBV
HCC
FXR/RXR Activation
Hepatic Fibrosis / Hepatic Stellate Cell Activat...
LXR/RXR Activation
Coagulation System
LPS/IL-1 Mediated Inhibition of RXR Function
PXR/RXR Activation
Role of NFAT in Regulation of the Immune Re...
IL-8 Signaling
Complement System
Extrinsic Prothrombin Activation Pathway
Estrogen Biosynthesis
Acute Phase Response Signaling
Axonal Guidance Signaling
Glioma Invasiveness Signaling
Atherosclerosis Signaling
Glucocorticoid Receptor Signaling
Antigen Presentation Pathway
Integrin Signaling
Acetone Degradation I (to Methylglyoxal)
IGF-1 Signaling
CD28 Signaling in T Helper Cells
Virus Entry via Endocytic Pathways
T Cell Receptor Signaling
NRF2-mediated Oxidative Stress Response
Role of Macrophages, Fibroblasts and Endoth...
Colorectal Cancer Metastasis Signaling
Gap Junction Signaling
Bupropion Degradation
Actin Nucleation by ARP-WASP Complex
CXCR4 Signaling
Histidine Degradation III
iCOS-iCOSL Signaling in T Helper Cells
Granulocyte Adhesion and Diapedesis
PKCθ Signaling in T Lymphocytes
Xenobiotic Metabolism Signaling
Phospholipase C Signaling
Molecular Mechanisms of Cancer
Role of Tissue Factor in Cancer
CTLA4 Signaling in Cytotoxic T Lymphocytes
Germ Cell-Sertoli Cell Junction Signaling
- log (p-val)
0.00
21.3
B)
Top up and downregualted genes in ´FXR/RXR activation pathway` pathway
NAFLD (0-1)
NAFLD (3-4)
HBV
HCC
PLTP
IL18
IL33
AE2
LPL
CETP
VLDLR
G6PC3
SLC51B
AKT1
SLCO1B1
CYP7A1
ORM1
TTR
A1BG
FETUB
HPR
ORM2
C9
APOF
Fold change
-23.37
16.10
C)
Top up and downregualted genes in ´LPS/IL-1 Mediated Inhibition of RXR Function` pathway
NAFLD (0-1)
NAFLD (3-4)
HBV
HCC
FABP4
PLTP
MD-2
IL18
IL33
ALDH1A3
FMO2
TNFRSF11B
FMO1
HS3ST3A1
NTCP
SLCO1B3
IL1RAP
CYP2C8
CYP7A1
c-Jun
CAR
CYP2C19
CYP3A7
CYP3A4
Fold change
-23.37
16.10
D)
Upstream regulators (IPA)
NAFLD (0-1)
NAFLD (3-4)
HBV
HCC
HNF4A
Interferon alpha
Alpha catenin
TGFB1
HNF1A
cardiotoxin
FOXM1
alefacept
tretinoin
pirinixic acid
PXR ligand-PXR-Retinoic acid-RXRα
rosiglitazone
aldesleukin
decitabine
IL2
nitrofurantoin
AHR
CD44
bicuculline
E. coli B4 lipopolysaccharide
IRF7
mono-(2-ethylhexyl)phthalate
IFNG
dalfampridine
Vegf
RETNLB
calcitriol
STAT1
methotrexate
lipopolysaccharide
PDCD1
HGF
HTT
HRG
SPI1
dexamethasone
L-dopa
trinitrobenzenesulfonic acid
CSF2
SREBF2
Activation z-score
-6.79
6.59

Click here to access/download
Supplementary Material
Supplement 4.xlsx

Click here to access/download
Supplementary Material
Supplement 5.xlsx

Click here to access/download

Supplementary Material

Supplement 7.xlsx

Click here to access/download

Supplementary Material

Supplement 10.xlsx

Click here to access/download

Supplementary Material

Supplement 15.xlsx

Point-by-point letter

Reviewer 1: The authors investigated time-dependent gene expression changes (gene networks) after CCl4-induced liver injury and recovery.

1. The authors provide a substantial amount of data on gene expression changes during injury and regeneration. Although this is a very comprehensive data collection, the results (early induction of stress- and inflammation-related genes and later upregulation of recovery genes) are not totally unexpected or new. The down-regulation of metabolism genes throughout the liver lobules is interesting. However, the study is certainly descriptive, and all conclusions rely mainly on correlations. It would be useful to include a paragraph at the end of the discussion that outlines some of the limitations including the fact that many of the gene changes may be of limited relevance for the overall pathophysiology and that specific interventions to modulate individual genes need to be applied to go beyond correlations and establish causality.

Response: We thank the reviewer for the helpful comments. As suggested a corresponding paragraph was added to the discussion.

2. A few minor issues need to be corrected:
a. P.14, line43 and p.15, line 35: references need to be numbered.
b. Figure 2: under biological motifs "pathway" is misspelled

Response: These errors were corrected.

Reviewer 2: The study done by Campos et al. presents the results of a trancriptomics analysis of mouse liver at eight time points after acute CCl4 intoxication. Their results were compared to others public studies (tunicamycin exposure, hepatocellular carcinoma, human chronic liver disease). Interestingly, a time-resolved transcriptional regulatory network (TRN) was performed, showing that CCl4 induced expression of genes for inflammation and stress signaling and concomitantly down regulated metabolic genes. In addition, the study showed that TRNs involved in the proliferation and restorative regeneration appear only later when metabolism is already suppressed.

The manuscript is well written and the study well established. All the data and analysis are accessible in the supplementary files, which is good. Therefore I recommend the manuscript for publication in archives of toxicology.

I have only minor comments that are described below:

P5 l17- Time series analysis on DILI chemicals have already been reported in previous studies and could be referred in the introduction (PMID:30279702; PMID:29085386). P6 l7- The author is using fuzzy clustering. If I am correct with a fuzzy clustering, a gene can belong to several clusters. So it means that high genes overlap can appear between clusters. Do the authors have an idea about the genes overlap between clusters? May be a small explanation on fuzzy clustering could be included on materials and methods.

Response: We thank the reviewer for this comment. The genes overlap between clusters is shown in the following table:

	Cluster 1a	Cluster 1b	Cluster 1c	Cluster 1d	Cluster 2a	Cluster 2b	Cluster 3a	Cluster 3b
Cluster 1a	**69.74%**	13.24%	5.12%	2.87%	2.83%	1.91%	1.54%	2.74%
Cluster 1b	7.33%	**73.17%**	15.49%	2.31%	0.76%	0.53%	0.19%	0.20%
Cluster 1c	1.56%	16.09%	**67.46%**	12.43%	1.16%	1.01%	0.16%	0.12%
Cluster 1d	1.28%	3.83%	15.54%	**66.29%**	5.66%	6.59%	0.52%	0.29%
Cluster 2a	0.67%	0.78%	1.32%	5.08%	**77.26%**	12.55%	1.82%	0.52%
Cluster 2b	0.99%	1.08%	1.88%	6.85%	17.57%	**67.99%**	2.76%	0.87%
Cluster 3a	0.70%	0.56%	0.61%	1.16%	3.78%	3.17%	**74.90%**	15.11%
Cluster 3b	1.39%	0.64%	0.44%	0.46%	0.93%	0.64%	14.47%	**81.04%**
Outlier	12.54%	13.69%	14.40%	14.94%	14.91%	13.51%	8.97%	7.03%

We added to materials and methods:

"Clusters of correlated genes based on similar time-dependent fold change after CCl_4 intoxication were generated by fuzzy c-means clustering with the fuzziness m=2. To cluster the gene expression profiles of DEGs, their profiles were logarithmised and scaled between the values -1 and 1. The optimal number of clusters was estimated using the 'Separation index'. A gene is assigned to the cluster with the highest degree of membership and if the maximum degree of membership is less than 0.3, the gene is regarded as unassignable and assigned to the group of outliers. A list with the genes contained in each cluster and the respective expression change can be found in the supplemental section."

P6 l29- The authors mentioned "NAFLD, score 0-1, 3-4". What means these scores?

Response: These are the clinically used standard scores to describe the severity of non-alcoholic fatty liver disease with 1 as the lowest and 4 the highest degree of steatosis.

P7 l15- If I understand correctly the PCA has been performed on 3750 genes. Do the authors see a similar trend using the full arrays?

Response: A pre-selection of genes is necessary to remove noise from the data set and to identify only relevant data matching the biological problem. A possible disadvantage of PCA is that by using the correlation matrix nonrelevant variables with low variance get a high impact on the analysis result.
Nevertheless, the PCA has been performed with higher and with lower numbers of probesets resulting in similar trends.

P7 l53- expression 8 and 24h -> expression at 8 and 24h

Response: The error was corrected; Thank you very much for making us aware.